Clim. Past, 20, 1327–1348, 2024
https://doi.org/10.5194/cp-20-1327-2024

Climate of the Past
Open Access
EGU

Late Eocene to early Oligocene productivity events in the proto-Southern Ocean and correlation to climate change

Gabrielle Rodrigues de Faria[1,2], David Lazarus[1], Johan Renaudie[1], Jessica Stammeier[3], Volkan Özen[1,2], and Ulrich Struck[1,2]

[1]Museum für Naturkunde, Leibniz Institute for Evolution and Biodiversity Science, Invalidenstraße 43, 10115 Berlin, Germany
[2]Freie Universität Berlin, Institute for Geological Sciences, Malteserstraße 74–100, 12249 Berlin, Germany
[3]GFZ German Research Centre for Geosciences, Telegrafenberg, 14473 Potsdam, Germany

Correspondence: Gabrielle Rodrigues de Faria (gabrielle.faria@mfn.berlin)

Received: 12 June 2023 – Discussion started: 25 July 2023
Revised: 29 February 2024 – Accepted: 22 April 2024 – Published: 14 June 2024

Abstract. The Eocene–Oligocene transition (EOT, ca. 40–33 Ma) marks a transformation from a largely ice-free to an icehouse climate mode that is well recorded by oxygen-stable isotopes and sea surface temperature proxies. Opening of the Southern Ocean gateways and decline in atmospheric carbon dioxide levels have been considered as factors in this global environmental transformation and the growth of ice sheets in Antarctica during the Cenozoic. A more comprehensive understanding is still needed of the interplay between forcing versus response, the correlation among environmental changes, and the involved feedback mechanisms. In this study, we investigate the spatio-temporal variation in export productivity using biogenic Ba (bio-Ba) from Ocean Drilling Program (ODP) sites in the Southern Ocean, focusing on possible mechanisms that controlled them as well as the correlation of export productivity changes to changes in the global carbon cycle. We document two high export productivity events in the Southern Ocean during the late Eocene (ca. 37 and 33.5 Ma) that correlate to proposed gateway-driven changes in regional circulation and to changes in global atmospheric pCO_2 levels. Our findings suggest that paleoceanographic changes following Southern Ocean gateway openings, along with more variable increases in circulation driven by episodic Antarctic ice sheet expansion, enhanced export production in the Southern Ocean from the late Eocene through early Oligocene. These factors may have played a role in episodic atmospheric carbon dioxide reduction, contributing to Antarctic glaciation during the Eocene–Oligocene transition.

1 Introduction

1.1 Late Eocene events as precursor to Antarctic Eocene–Oligocene boundary glaciation

The Eocene–Oligocene transition (EOT, ca. 40–33 Ma) is the most important climatic interval of the Cenozoic era (Westerhold et al., 2020). This interval involves profound transformations in environmental conditions including the onset of continental-scale Antarctica glaciation at the Eocene–Oligocene boundary (Shackleton and Kennett, 1975; Zachos et al., 1996; Coxall et al., 2005), sea level fall (Houben et al., 2012), and global cooling (Prothero and Berggren, 1992; Liu et al., 2009; Bohaty et al., 2012; Hutchinson et al., 2021), as evidenced by a global shift in oxygen isotope records from biogenic calcium carbonate ($> 1‰$; Zachos et al., 2001; Coxall et al., 2005; Bohaty et al., 2012; Westerhold et al., 2020). A positive deep-sea carbon isotope excursion of up to 1 ‰ (Zachos et al., 2001; Coxall et al.,. 2005; Coxall and Wilson, 2011; Westerhold et al., 2020) and a change from a shallow (~ 3.5 km) to a deeper (~ 4.5 km) calcite compensation depth (CCD) (Coxall et al., 2005; Rea and Lyle, 2005; Pälike et al., 2012; Dutkiewicz and Müller, 2021; Taylor et al., 2023) have also been observed and indicate that the carbon cycle played an important role in the changes observed during the transition, although the mechanisms that caused the carbon cycle perturbation are still unsolved.

Carbon cycling acts through a variety of feedback mechanisms. Even though it is well recognized that changes in atmospheric carbon dioxide (CO_2) impact the Earth's climate

because of its large effect on temperature (Arrhenius, 1896; IPCC, 2021), the mechanisms controlling CO_2 levels over long timescales are still a matter of debate. A simplified carbon cycle theory suggests that the level of CO_2 is expected to remain in a steady state over multi-millennial (> 10 kyr) timescales (Berner et al., 1983; DeVries, 2022). This stability is attributed to a dynamic interplay of transfer of carbon between volcanic inputs, oceans, atmosphere, and sequestration in marine sediments involving several mechanisms such as weathering, volcanism, and the ocean's biological pump.

However, the Earth's pCO_2 has, in fact, undergone substantial changes, from glacial–interglacial timescales (Sigman and Boyle, 2000) to long-term changes during the Cenozoic (Beerling and Royer, 2011; Anagnostou et al., 2016), thus suggesting that the Earth's carbon system operates in a more complex way than proposed in the canonical model.

Changes in the Southern Ocean productivity are thought to have altered pCO_2 levels in the Earth's past, specifically on glacial–interglacial timescales (Archer et al., 2000; Sigman et al., 2010), although magnitude and timing remain debated. Changes in the late Eocene Southern Ocean export productivity over 1 million years, as documented in our research, could potentially have impacted CO_2 levels, as hypothesized by Egan et al., (2013) based on Si isotope proxy data for Paleogene Southern Ocean diatom productivity.

The carbon cycle perturbation at the EOT provides an opportunity to understand climate–carbon cycle feedback (Zachos and Kump, 2005). The mechanisms proposed to explain such perturbations are processes operating gradually over long timescales and may have had their origins in the middle to late Eocene. Preceding the abrupt change at the E–O boundary, the late Eocene was a period of gradual cooling and progressive CO_2 levels decrease (Lauretano et al., 2021). The events associated with this time period may have had substantial importance in pre-conditioning the climate system prior to the major climatic shift at the E–O boundary (Egan et al., 2013). The potential main drivers for the initiation of this global cooling and ice build-up in Antarctica are actively debated. Declining global atmospheric carbon dioxide concentrations, and the opening of Southern Hemisphere oceanic gateways, namely the Drake Passage (DP) and the Tasmanian Gateway (TG), are often proposed hypotheses to explain this transition (Coxall and Pearson, 2007; DeConto et al., 2008). The decline in carbon dioxide levels is an important factor in driving cooler temperatures and has been suggested as the crucial factor in the EOT cooling and subsequent build-up of continental glaciers on Antarctica (DeConto and Pollard, 2003; Huber and Nof, 2006; Pagani et al., 2011). Atmospheric CO_2 partial pressure (pCO_2) decline has robust observational support. Atmospheric pCO_2 has been shown to decline through the Eocene, from ca. 1400 ppm at the Early Eocene Climate Optimum (EECO, ca. 51 to 53 million years ago) to about 770 ppm in the late Eocene, reaching a minimum of 550 ± 190 ppm in the early Oligocene (Anagnostou et al., 2016). However, data are noisy, with significant variations among different proxies, and thus details of the magnitude and timing are still unclear. Furthermore, the CO_2 threshold (~ 780 ppmv) needed for the onset of Antarctica glaciation is highly dependent on model boundary conditions while ice sheet model simulations reveal inter-model disagreement (Gasson et al., 2014). Therefore, it is crucial to approach this leading hypothesis with caution due to these uncertainties.

The tectonic opening of the Southern Ocean gateways is considered a mechanism contributing to the climatic shift because it allows the initiation of a circum-Antarctic flow, leading to the formation of the Antarctic Circumpolar Current (ACC) (Kennett, 1977; Barker, 2001; Scher and Martin, 2006; Toumoulin et al., 2020). This intense eastward-flowing current is proposed in this hypothesis to impact the regional and global climate by preventing tropical heat of low latitudes from reaching Antarctica, promoting the thermal isolation of Antarctica. Numerous ocean circulation model studies of this hypothesis have yielded conflicting results (Mikolajewicz et al., 1993; Najjar et al., 2002; De Conto and Pollard, 2003; Sijp et al., 2009; Goldner et al., 2014; Ladant et al., 2014; Inglis et al., 2015) but most of these earlier works were limited by unrealistic boundary conditions or other issues (Toumoulin et al., 2020; Hutchinson et al., 2021). Recent modelling circulation studies (e.g. Toumoulin et al., 2020; Sauermilch, et al., 2021) demonstrate the importance of the southern gateway openings and the proto-ACC on ocean cooling in the Southern Hemisphere. Additionally, glaciation has itself been a strong influence both on the circulation of the Southern Ocean and on global climate via increased albedo, colder temperatures, increased latitudinal temperature gradients, and stronger zonal winds (Goldner et al., 2014). There is increasing evidence for at least partial, if transient, Antarctic continental glaciation within the late Eocene (Scher et al., 2014), and thus this also needs to be considered in understanding how climate and ocean change developed within this period.

In addition to the above physical impacts, the ACC is associated with the development of the Southern Ocean fronts that contribute to upwelling-induced biological productivity (Chapman et al., 2020). Considering that the changes in the Southern Ocean circulation have the potential to affect export productivity and via its link to carbon sequestration in sediments, in removing CO_2 from the ocean–atmosphere system, the "CO_2" hypothesis and the "tectonic" hypothesis may be linked via the influence that gateways may have had on Southern Ocean circulation, increasing export productivity enough to affect global pCO_2 (Egan et al., 2013). Therefore, evaluating export productivity patterns in the Southern Ocean across the Eocene–Oligocene and its relationship with circulation and decline of atmospheric carbon dioxide during this time period provide important information about possible climate feedbacks in this prominent climatic transition.

Many studies have shown variations in biological productivity during this time interval (Diester-Haass, 1995; Diester-

Haass and Zahn, 1996, 2001; Salamy and Zachos, 1999; Diester-Haass and Zachos, 2003; Schumacher and Lazarus, 2004; Anderson and Delaney, 2005; Villa et al., 2014), pointing towards a productivity increase associated with ocean circulation changes that increased surface water nutrient availability (Diester-Haass, 1992; Zachos et al., 1996). However, existing studies have mostly focused on single sites, whose paleoceanographic history may reflect local rather than regional developments. A much broader spatial investigation is particularly important for understanding the influence of large-scale ocean circulation on this process. Moreover, the timing of productivity changes differs among the studies and different proxies, limiting our understanding of cause-and-effect relationship. This highlights the importance of well-constrained age models and use of consistent paleoproductivity proxies.

Here, we reconstruct changes in export productivity in the Southern Ocean across the late Eocene and early Oligocene and evaluate how the changes observed may be linked to ocean circulation changes and how they may have contributed to the climate changes observed at this interval. We utilize biogenic barium (bio-Ba) accumulation rates to measure marine export productivity. Bio-Ba is defined as the fraction of total barium that is not associated with terrigenous sources, sometimes referred to as excess-Ba (Dymond et al., 1992), and has been applied in several studies in the Paleogene (e.g. Nielsen et al., 2003; Anderson and Delaney, 2005; Faul and Delaney, 2010). It is considered a relatively reliable proxy to estimate changes in paleoproductivity in the Southern Ocean. Newly generated carbon and oxygen-stable isotope records from the same samples of our bio-Ba data further constrain possible causative mechanisms for the climatic shift at the EOT. We compare our export productivity proxy results to indicators of ocean circulation change, such as neodymium (Nd) isotopes. Neodymium isotopes have emerged as a valuable geochemical water mass tracer (Piepgras and Wasserburg, 1982; Martin and Haley, 2000; Roberts et al., 2010), contributing significantly to our understanding of the role of ocean circulation in the geological past. This proxy provides an opportunity to assess the origin of water masses and reconstruct deep-ocean circulation. Here, we use Nd isotope data to help understand gateway opening, paleoceanographic changes, and ice sheet history during the Eocene–Oligocene transition, and how these changes may have influenced marine biological productivity. We also compare our productivity records to well-established proxies for the global carbon cycle, specifically pCO_2 and $\partial^{13}C$ of benthic deep-sea foraminifera.

Our understanding of the Eocene–Oligocene transition has been enhanced through modelling studies as they provide means to compare several possible scenarios and generate "data" for components of the system for which no direct proxy data are available. However, all models are simplifications of complex and not fully understood systems and are dependent on parameterizations and calibrations to often sparse, noisy proxies that ground truth model outputs. This paper instead focuses on proxy evidence of the changes that occurred in this time interval.

1.2 Paleoceanographic setting

The Southern Ocean (SO) today is an important part of the global ocean circulation and climate system, interconnecting the Atlantic, Pacific, and Indian ocean basins and thus providing inter-basin exchange of ocean properties and heat (Rintoul et al., 2001). There are strong latitudinal gradients and seasonal changes in ocean properties which affect surface water and export productivity, and thus this region's role in global carbon capture and sequestration. Low light levels and, at higher latitudes, extensive sea ice limit productivity during the winter months. Deep surface mixed layers over the large areas of the Southern Ocean, beyond the shallow stratification effects of meltwater near the sea ice edge, also tend to limit productivity in spring through fall as plankton is mixed below critical thresholds of light availability (Deppeler and Davidson, 2017). The relationship between mixed-layer thickness and productivity, however, is complex (Nelson and Smith, 1991; Li et al., 2021). Southern Ocean productivity is thus concentrated near the Antarctic Circumpolar Current (ACC), the dominant current in the region. This current is the longest and strongest ocean current on Earth. This complex circulation system is driven mainly by westerly winds, resulting in Ekman transport and favouring deep-water upwelling. This flow pattern is possible in the absence of land barriers and is governed by bathymetry (Rintoul et al., 2001; Carter et al., 2008), while the strength of the current is driven by the strength and location of the westerly winds, and thus, among other factors, the global latitudinal thermal gradient. The ACC is a key component of the "ocean conveyor belt", playing a role in the global transport of heat (Rintoul et al., 2001; Katz, et al., 2011). Moreover, this circumpolar current influences the strength of meridional overturning circulation, and several authors have proposed that this current is one of the main drivers of the Atlantic Meridional Overturning Circulation (AMOC) (Toggweiler and Samuels, 1995; Toggweiler and Bjornsson, 2000; Scher and Martin, 2006; Kuhlbrodt et al., 2007; Scher et al., 2015; Sarkar et al., 2019).

The ACC is structured of multiple hydrological fronts, associated with specific water mass properties such as temperature and salinity (Sokolov and Rintoul, 2009). Orsi et al., 1995 proposed the traditional view of Southern Ocean fronts. It consists of the Subantarctic Front (SAF), the Antarctic Polar Front (APF), and the Southern ACC Front (SACCF). Besides these main fronts, a Subtropical Frontal Zone (STFZ) can be found north of the ACC (Orsi et al., 1995; Palter et al., 2013; Chapman et al., 2020). This frontal structure is fundamental to different processes that occur in the region, such as the distribution of important nutrients through the exchange between deep and surface ocean, and the ex-

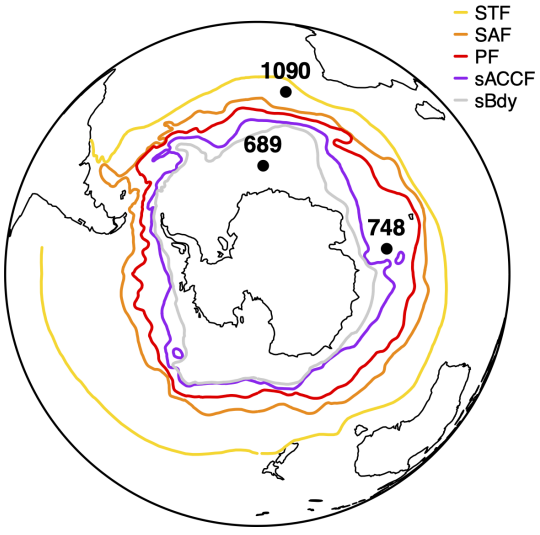

Figure 1. Schematic Antarctic Circumpolar Current (ACC) and Southern Ocean fronts as determined by Orsi et al. (1995) named, from north to south, Subtropical Front (STF), Subantarctic Front (SAF), Polar Front (PF), Southern Antarctic Circumpolar Current Front (SACCF), and Southern Boundary Front (sBdy). Modern location of ODP sites (1090, Agulhas Ridge; 689, Maud Rise; and 748, Kerguelen Plateau) used for reconstructions in this study. ODP stands for Ocean Drilling Program.

change of tracers (Palter et al., 2013). Upwelling of Circumpolar Deep Water (CDW) brings nutrient-rich waters to the surface towards the Polar Front Zone (PFZ) where Antarctic Surface Waters (AASW) sink to form Antarctic Intermediate Water (AAIW); thereafter, it extends into the Subantarctic Zone (SAZ) (Sarmiento et al., 2004) (Fig. 1).

Wind-driven upwelling that occurs within the Southern Ocean fronts enhances biological productivity in these regions (De Baar et al., 1995; Moore et al., 1999). More recently, upwelling related to ACC bathymetry has been found as an important mechanism for establishing phytoplankton blooms in the SO (Sokolov and Rintoul, 2007). This complex structure involving ACC fronts, westerlies and the bottom topography, makes the Southern Ocean a highly productive region. Iron remobilization has also been shown to occur due to latitudinal variations of the ACC (Kim et al., 2009), inducing increases in productivity.

The conventional assumption is that the ACC structure began to develop during the Cenozoic, with the opening of the Southern Ocean pathways between South America and Antarctica and the following formation of the Drake Passage (DP) and also between Australia and Antarctica that allows the Tasmanian Gateway (TG) opening. Removing these geographic barriers permitted a gradual development of circumpolar flow (Toggweiler and Bjornsoon, 2000). The TG opening to intermediate and deep waters occurred in the late Eocene, ca. 35.5 Ma (Stickley et al., 2004). In contrast, tectonic reconstructions for the timing of the Drake Passage opening remain controversial, ranging from the late Eocene (ca. 41 Ma; Scher and Martin, 2004, 2006) to the late Oligocene (ca. 26 Ma, Barker and Thomas 2004; Hill et al., 2013) for shallow-water exchange. Some studies pointed to deep-water exchange occurring as late as the earliest Miocene (ca. 22–23 Ma, Barker 2001; Lyle et al., 2007). Even if the timing of the deepening of the Drake Passage is less well constrained, a "proto-ACC" has been proposed as an earlier expression of the ACC, and it is defined as a shallow-depth circumpolar current (Scher et al., 2015; Sarkar, et al., 2019). Cramer et al. (2009) suggested that "proto-ACC" would have played an important role in the ocean circulation changes that occurred in the Eocene. Furthermore, even a relatively shallow proto-ACC would have strongly affected surface water phytoplankton and zooplankton (Lazarus and Caulet, 1994) and thus potentially the mechanisms of surface water productivity in the region.

Many climate model studies have contributed insights into the ocean structure and circulation of the late Eocene (e.g. Huber et al., 2004; Huber and Nof, 2006; Sijp et al., 2011, 2016; Elsworth et al., 2017; Baatsen et al., 2020; Toumoulin, et al., 2020; Sauermilch et al., 2021; Nooteboom et al., 2022). Although some of these experiments have shown that opening of gateways was not sufficient to have caused the global cooling recorded by proxies (DeConto and Pollard, 2003; Huber et al., 2004; Huber and Nof, 2006; Sijp et al., 2011; Baatsen et al., 2020), they acknowledge that the circulation patterns have changed during the Eocene. A recent model circulation experiment has demonstrated a significant regional impact of the DP opening and its effects on ocean structure and dynamics even for shallow depths (Toumoulin et al., 2020).

The organization of Southern Ocean proto-oceanic fronts may have occurred during the late Eocene as shown by microfossil biogeographic data (Lazarus and Caulet, 1994; Cooke et al., 2002). This frontal system organization likely played a role in major changes at that time period, including higher ocean productivity.

Evidence of significant events during the late Eocene highlights the importance of this period that preceded the permanent glaciation in Antarctica. An interval of increasingly heavy global benthic oxygen isotope values in the late Eocene, at ca. 37 Ma have been interpreted to reflect pre-EOT glaciation and cooling, this episode is referenced as PrOM event (Priabonian Oxygen Isotope Maximum, Scher et al., 2014). Additional evidence for a prominent cooling episode has been found during this time period (Anderson et al., 2011; Douglas et al., 2014). Despite uncertainties about the nature and extent of the earliest ice in Antarctica, these changes imply that paleogeographic reconfiguration has affected the late Eocene Antarctic climate, and it is likely that a combination of processes favoured the development of permanent glaciation in Antarctica.

Given the importance of changes during the Eocene–Oligocene time interval, especially the ACC development

Table 1. Position of the ODP sites studied in the present day and in the late Eocene (∼ 37 Ma). Paleocoordinates are calculated based on Seton et al. (2012) rotation model.

Site	Geographic Setting	Latitude	Longitude	Water depth (m)	Paleodepths (m)	Paleo-latitude	Paleo-longitude
1090	Agulhas Ridge	42°54.8′ S	8°53.9′ E	3702	ca. 3000–3300 (Pusz et al., 2011)	ca. 47°33′ S	ca. 1°46.8′ E
689	Maud Rise	64°31′ S	3°6′ E	2253	ca. 1500 (Diester-Haass and Zahn, 1996)	ca. 64°19.2′ S	ca. 2°43.2′ E
748	Kerguelen Plateau	58°26.45′ S	78°58.89′ E	1290.9	ca. 1200 (Wright et al., 2018)	ca. 56°48.6′ S	ca. 75°36′ E

and its frontal structure to the climate system and ecosystems, it is crucial to investigate the timing and magnitude of late Eocene paleoceanographic changes in the Southern Ocean, and it is equally important to expand our understanding of the implications of such changes on paleoproductivity and how these mechanisms are linked to a changing climate.

Our multiproxy approach and wide coverage allow us to test the following hypotheses.

Hypothesis one (H1) is that changes in ocean circulation patterns that took place during the late Eocene and early Oligocene (e.g. development of a proto-ACC and strengthening of AMOC) contributed to the increase in biological productivity in the Southern Ocean.

Hypothesis two (H2) is that the export productivity increase that preceded the EOT may have been temporally correlated with (and thus may have contributed to) the drawdown of pCO_2.

First, we investigate the export productivity changes across the late Eocene to early Oligocene in three different regions in the Southern Ocean. We then compare our results to the paleo-circulation changes that occurred in the same time period, and we lastly compare our productivity records to the temporal pattern of change in Eocene–Oligocene pCO_2. We conclude by summarizing the implications of the changes in ocean circulation and the possible climate-driving mechanisms that led to the cooling of the Earth.

2 Materials and methods

2.1 Site descriptions

We investigated sediment samples from three Ocean Drilling Program (ODP) sites in the Southern Ocean (Table 1). ODP Site 1090 on the southern flank of the Agulhas Ridge in the southern Atlantic Ocean (42°54.8′ S, 8°53.9′ E, water depth 3702 m), ODP Site 689 on the southern flank of the Maud Rise in the southern Atlantic Ocean (64°31′ S, 3°6′ E, water depth 2253 m), and ODP Site 748 on the southern part of the Kerguelen Plateau in the southern Indian Ocean (58°26.45′ S, 78°58.89′ E, water depth 1290.9 m). All the sites lie on topographic highs. The Agulhas Ridge comprises an elongate part of the Agulhas–Falkland Fracture Zone (AFFZ). The ridge rises ∼ 3000 m above the surrounding floor and constitutes a topographic barrier, having a strong influence on the exchange of water masses (Gruetzner and Uenzelmann-Neben, 2016) between high and lower latitudes. The Maud Rise is a seamount, its elevation rises almost 3000 m from the seafloor (Brandt et al., 2011). Kerguelen Plateau is a large topographic high in the Indian sector of the Southern Ocean. We selected samples from the middle Eocene through the E–O boundary, depending on the sample availability.

Currently, the sites studied are located in the Southern Ocean through the ACC. Site 689 is located well south of the Polar Front Zone (PFZ), Site 748 is located slightly to the south of the PFZ, and Site 1090 is located in the subantarctic zone, between the Subtropical Front (STF) and the Subantarctic Front (SAF) (Fig. 1). Across the Eocene–Oligocene transition, the sites were shallower (Table 1), ranging between ca. 1.2 and 3 km paleo water depth. These depths are well suited to capture signals of export productivity to intermediate-depth waters. The locations of Site 689 and Site 748 locations were similar to today, while Site 1090 was as much as 5° farther to the south (Gersonde et al., 1999) (Table 1).

The major lithology from the lower Eocene to the upper Oligocene at the Maud Rise is composed of calcareous and silicious oozes (Barker et al., 1988). The Kerguelen Plateau site is composed mainly of nannofossil ooze and chert (Barron et al., 1989). The Agulhas Ridge is predominantly composed of diatoms and nannofossil ooze, with $CaCO_3$ wt % highly variable, ranging from non-detectable to 69 % of sediment throughout the study interval (Gersonde et al., 1999) with rare occurrences and barren intervals of planktic and benthic foraminifera making it difficult to establish stable isotope records at this site.

2.2 Age models and linear sedimentation rates

Revised age models for the ODP Site 1090, ODP Site 689, and ODP Site 748 made for this study were based on all magnetostratigraphic and biostratigraphic data available,

and both models and data are available from the Neptune database (NSB) system (Renaudie et al., 2020) (Figs. S1–S4 in the Supplement). All ages in our study are given in the geomagnetic polarity timescale (GPTS) standard used by NSB (Gradstein et al., 2012) or have been remapped to this scale from prior studies. Differences between this and more recent GPTS scales in the Cenozoic are minor, and generally lower than other age model uncertainties for the sections in our study.

ODP Site 1090 has an age model constructed from shipboard magnetostratigraphic "U-channel" measurements, and the records fit well to the GPTS (Channell et al., 2003). Nannofossil biostratigraphy has confirmed the Chron ages (Marino and Flores, 2002), foraminiferal biostratigraphy (Galeotti et al., 2002), strontium isotopes (Channell et al., 2003), and oxygen and carbon isotope data from benthic foraminifera (Zachos et al., 2001; Billups et al., 2002). This integration of several age indicators and their consistency makes this a robust and very well-constrained age model.

Magnetostratigraphic data for ODP Site 689 are partially reinterpreted from the measurements originally made by Spiess (1990). A new high-resolution study of Eocene–Oligocene "U-channel" samples from this site shows a high correlation with the GPTS (Florindo and Roberts, 2005). Calcareous nannofossil datums (Wei and Wise, 1992; Wei, 1992; Persico and Villa, 2004), planktonic foraminiferal datums (Kennett and Stott, 1990; Thomas, 1990; Berggren et al., 1995), and argon–argon ($^{40}Ar/^{39}Ar$) dating (Glass et al., 1996; Vonhof et al., 2000) are used to re-calibrate ages for this site.

A high-resolution magnetostratigraphic study from ODP Site 748B was carried out by Roberts et al. (2003) in continuous "U-channel" samples, revising the shipboard analysis from Inokuchi and Heider (1992). Calcareous nannofossil biostratigraphy (Aubry, 1992), planktonic foraminiferal biostratigraphic datums (Berggren et al., 1995), diatom datums (Baldauf and Barron, 1991; Roberts et al., 2003), and strontium isotope ages (Zachos et al., 1999; Roberts et al., 2003) were re-evaluated for a better age model.

Accumulation rate fluxes are obtained by calculating the product of linear sedimentation rates (LSRs) and shipboard measured dry bulk densities (DBDs); thus, a robust age model is crucial for this calculation because it determines the linear sedimentation rates. We use a straightforward LSR calculation between age–depth control points based on magnetostratigraphic data, stable isotopes, and biostratigraphic data. Mass accumulation rates (MARs, $mol\,cm^{-2}\,kyr^{-1}$) were calculated using LSR based on the above age models multiplied by DBD.

Since bio-Ba accumulation rate (AR) is a direct function of LSR, it is essential to evaluate any possible biases due to this. Figure S5 shows a comparison of linear sedimentation rates and bio-Ba AR. This comparison showed a high-amplitude peak at ODP Site 1090, with LSR of $4.11\,cm\,kyr^{-1}$ at the late Eocene, this high rate is based on a very constrained model. The LSRs for ODP Site 689 vary from $0.1\,cm\,kyr^{-1}$ during the early Oligocene to up to $1.3\,cm\,kyr^{-1}$ in the late Eocene, whereas ODP Site 748 has more uniform values during the late Eocene. The available age data for our sites allow some variation in the placement of the line of correlation, and thus the precise timing and magnitude of sedimentation rate changes on the scale of $\pm$ ca. 0.5 Myr are not well constrained. Patterns and calculated values over longer timescales are, however, thought to be robust.

2.3 Stable isotope analyses

Stable isotopes of carbon and oxygen were measured both on the bulk fine fraction ($< 45\,\mu m$) and benthic foraminifera. Bulk sediments were oven-dried and washed through different sieve sizes (125 and 45 µm). Smear slide observations indicate that the main carbonate composition of the fine fraction is coccoliths; therefore, stable isotopic compositions of bulk fine fraction ($< 45\,\mu m$) reflect primarily nannofossil isotope signals. Contamination by non-coccolith carbonate such as fragments of foraminifera shells is minimal (Fig. S5). A total of 15 to 20 tests of benthic foraminifera (*Cibicidoides* spp.) were picked from the $> 125\,\mu m$-size fraction. Foraminiferal tests were ultrasonically cleaned using ethanol and oven-dried. Stable isotopic analyses were carried out at the Stable Isotope Laboratory of the Museum für Naturkunde (Berlin, Germany) on a thermo-isotope ratio mass spectrometer. All values are reported in the δ notation in parts per million (‰) relative to the Vienna Pee Dee Belemnite (VPDB). In this study, we applied an adjustment of +0.64 ‰ (Shackleton and Opdyke, 1973; Shackleton et al., 1984) to all $\delta^{18}O$ values of the benthic foraminifera *Cibicidoides* to account for disequilibrium effects.

2.4 Barium analyses and biogenic barium as a paleoproductivity proxy

Barium (Ba) and aluminium (Al) were analysed by inductively coupled plasma optical emission spectrometry (ICP OES), performed at the ElMiE Lab at the German Centre for Geosciences (GFZ, Potsdam, Germany) using a 5110 spectrometer (Agilent, USA). The analytical precision and repeatability were generally better than 2 %, and it is regularly tested by certified reference material and in-house standards. For preparation, 2 g of each sample was grounded to assure grain size distribution and digested by Na_2O_2 fusion and HCl using ultrapure reagents, following the method by Bokhari and Meisel (2016). Intensity calibration was performed by external calibration using the same batch of solvent to ensure matrix matching. The analytical blank was negligible compared to the sample concentration.

Using barium as a paleoproductivity proxy requires some adjustments because other biogenic sources may contribute to the barium content in the sediment. Detrital aluminosilicate may affect the barium signal in Southern Ocean sedi-

ments. In order to solve this issue and reveal aluminosilicate contributions, the biogenic barium calculation was used as proposed by Dymond et al., 1992, following Eq. (1).

$$\text{Biogenic Barium (Bio Ba)} = (\text{Ba-total})_{\text{sample}} - (\text{Ba/Al})_{\text{bulk continental crust}} \times \text{Al}_{\text{sample}} \quad (1)$$

This assumes that the aluminium (Al) concentration and the average continental crust abundance are representative of the detrital Ba component. The Ba/Al crust ratio of 0.0075 is the global average value from sedimentary rocks as suggested by Dymond et al. (1992). This value is based on various compilations of elemental abundances in crustal rocks. This normative calculation potentially introduces uncertainty in samples with high and variable detrital barium, but considering that clay assemblages and weathering regimes were relatively constant during the early Paleogene in the Southern Ocean, the crustal ratio therefore probably did not vary much (Robert et al., 2002).

2.5 Data compilation

2.5.1 Neodymium isotope data

Neodymium isotopes in seawater reflect the different weathering sources of neodymium that affect each water mass. The isotope values act as conservative elements during ocean mixing. They are therefore a robust water mass tracer, and are faithfully archived in sediments (Piepgras and Wasserburg, 1982; Martin and Haley, 2000). Their behaviour in seawater and the conservation of the signal in sediments make them a valuable proxy for paleoceanographic studies and past ocean circulation reconstruction. Fossilized fish teeth are commonly used and considered robust archives to extract Nd isotopic signatures because they incorporate and preserve their Nd signature during very early diagenesis (Martin and Scher, 2004), and they can be found in deep-sea sediment samples all over the world and in many geologic time intervals. The Nd signal is given in εNd, where εNd is the ratio $^{143}Nd/^{144}Nd$ of a sample relative to the same of the bulk Earth in parts per 10 000.

In this study, we compiled published Nd isotope data from fossil fish teeth, from the same Ocean Drilling Program (ODP) sites that we investigated in the Southern Ocean (ODP Site 1090 on Agulhas Ridge, Scher and Martin, 2006; ODP Site 689 on Maud Rise, Scher and Martin, 2004; and ODP sites 738, 744, and 748 on the Kerguelen Plateau, Scher and Delaney, 2010; Scher et al., 2011, 2014; Wright et al., 2018) and explore the Nd isotope variability to examine the intrusion of waters from the Pacific to the Atlantic sector of the Southern Ocean. We then used these data and our records to explore the evolution of the Southern Ocean circulation and significant circulation changes across the Eocene–Oligocene transition. Sources of Nd isotope data are given in Table S1 in the Supplement.

2.5.2 pCO_2 data

A variety of geological proxies have been applied in numerous studies to reconstruct the partial pressure of atmospheric CO_2 (pCO_2) during the Cenozoic Era (e.g. Pagani et al., 2005, 2011; Kürschner et al., 2008; Retallack., 2009; Beerling and Royer 2011; Anagnostou et al., 2016, 2020). Given the low published sampling density through the critical Eocene–Oligocene interval, we compiled published pCO_2 data from marine and terrestrial proxies that have been identified as reliable for reconstructing pCO_2 during this period. The marine geochemical proxies include alkenone-based estimations and carbon and boron isotope ($\delta^{11}B$) compositions of well-preserved planktonic foraminifera calcite. Proxies from the terrestrial reservoir include paleosols and stomatal frequencies. Our atmospheric CO_2 compilation (Table S2) consists to our knowledge all the currently available proxy data on Eocene and Oligocene pCO_2 records, including all data compiled in previous syntheses through extensive scientific community efforts in paleo CO_2 database (The Cenozoic CO_2 Proxy Integration Project Consortium, 2023), such compilations are commonly used to estimate past pCO_2, although it is known that there are limitations and variation among them (IPCC, 2021). Zhang et al. (2013) specifically argued that compositing limited, short-time-interval data from different proxies and different localities is likely to introduce significant short-term bias at individual data series end-points into the resulting fitted curve, and instead generated a 40 Myr long history of Cenozoic pCO_2 using a single proxy from a single section (Site 925 in the equatorial Atlantic). We consider this study's results to be the best and most complete single source of information on the Cenozoic trend of atmospheric pCO_2. However, precisely because of the substantial amounts of between proxies and between locality variation, data using a single proxy and from a single site is also potentially not representative of global pCO_2 history. We thus use both the single site results of Zhang et al. (2013) and the full, multi-site, and multi-proxy compilation (Supplement) in evaluating our own study's results.

3 Results

3.1 Biogenic barium

Biogenic barium accumulation rate (bio-Ba AR) records (Fig. 2) show a pronounced rise in the late Eocene when the values were up to twice as high as in previous periods for all sites studied. At Kerguelen Plateau ODP Site 748, we also observe a previous and smaller increase around the middle Eocene Climatic Optimum (MECO, ca. 40 Ma). At Maud Rise the increase began at ca. 38.3 Ma and persisted for around 1.5 Myr. Bio-Ba ARs show a high value in the Agulhas Ridge at ca. 36.8 Ma which is induced by a high sedimentation rate (Fig. S5a). Although export productivity was higher (maximum values to about

16.8 µmol bio − Ba cm^{-2} kyr^{-1}) at Maud Rise compared to the other sites, the Kerguelen Plateau reached maximum values of about 14.3 µmol cm^{-2} kyr^{-1} and the Agulhas Ridge site 13.74 µmol cm^{-2} ky^{-1}, the records show a high degree of temporal correspondence in the late Eocene peak (ca. 36.8 Ma). Bio-Ba values were low at all sites between ca. 36 and 34.5 Ma. Between ca. 34.5 Ma and ca. 33.3 Ma, which includes the EOT interval, bio-Ba AR increased in both sites of the Atlantic sector, but these increases were not very concurrent between the sites investigated. On the Agulhas Ridge, ODP Site 1090, the rise in bio-Ba (from 7.37 to 20.46 µmol cm^{-2} kyr^{-1}) is observed in the very latest Eocene (ca. 34.3), just before the Oi-1 event. At Maud Rise, ODP Site 689, the increase is not observed until ca. 1 Myr after, in the early Oligocene (maximum value 16.25 µmol cm^{-2} kyr^{-1} at ca. 33.3 Ma). On the Kerguelen Plateau, ODP Site 748, the increase in export productivity registered by bio-Ba during the Oligocene is notably smaller than in the Atlantic sites, with values not higher than the low values observed during the Eocene.

Our bio-Ba results are in general concordant with the temporally more limited data obtained by prior studies of Southern Ocean sites (Anderson and Delaney, 2005, Site 1090; Diester-Haass and Faul, 2019, Site 689) (Fig. 2). However, our results for Kerguelen Plateau Site 748 differ from those of Faul and Delaney (2010) for nearby Site 738, where the latter estimate bio-Ba accumulation rates up to twice those obtained in our study of Site 748. The differences may be due to the different locations of the two sites, Site 738 is located several degrees further south and at ca. 1 km deeper water depth. The bio-Ba proxy is also very sensitive to sedimentation rates, and the differences may be due to the poor age control for Site 738, which in the studied time interval consists only of a few rather scattered biostratigraphic events (Fig. S4a), resulting in substantially different age models between our study, Faul and Delaney (2010), and other recent studies of this site, e.g. Huber and Quillevere (2005). In these studies the location and extent of hiatuses and the uniformity of sedimentation rates varies considerably (SOM Fig. S4b). The age model for Site 748 by contrast (Fig. S3) is very well constrained by coherent biostratigraphic events from multiple groups of microfossils, Sr isotope stratigraphy, and paleomagnetic stratigraphy, and we therefore accept the results from Site 748 as being more reliable.

When the data for individual sites are composited together, the behaviour of the Southern Ocean region can be roughly estimated, even though our geographic coverage (lacking data from the Pacific–New Zealand sector) is incomplete and thus may not be entirely representative of the Southern Ocean as a whole. A lowess curve fit to the composited bio-Ba data shows that the key patterns noted in individual records are retained in the composite signal, and thus that Southern Ocean productivity can be characterized as having had two intervals of high values at around 37 and 34 Ma.

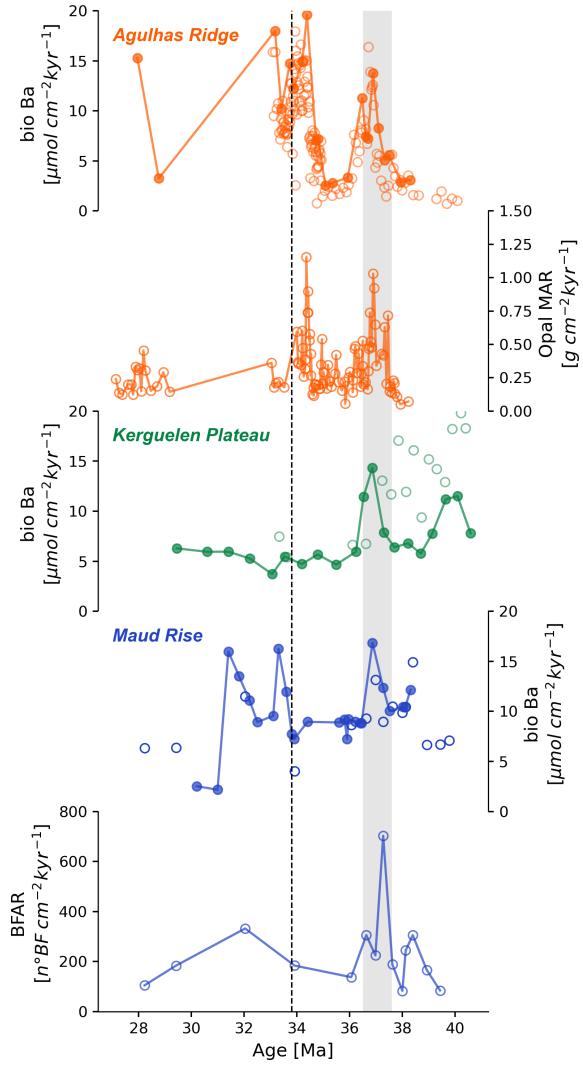

Figure 2. Paleoproductivity proxies versus age (Ma) for Agulhas Ridge (ODP Site 1090, in orange), Maud Rise (ODP Site 689, in blue), and the Kerguelen Plateau (ODP sites 748, 744, in green). Solid circles are new biogenic barium accumulation rate (bio-Ba, µmol cm^{-2} kyr^{-1}) data of this study, open circles are those from prior literature (Agulhas Ridge data from Anderson and Delaney, 2005; Maud Rise data from Diester-Haass and Faul, 2019; Kerguelen Plateau data from Faul and Delaney, 2010). Site 1090 opal MAR data are from Diekmann et al. (2004). Site 689 BFAR data are from Diester-Haass and Faul (2019). The vertical dashed line identifies the E–O boundary (at ca. 33.8 Ma). The shaded area encompasses the late Eocene productivity event.

3.2 Oxygen and carbon isotopes

Our new oxygen (Fig. 3c and e) and carbon (Fig. 3d and f) stable isotope data allow us to identify previously noted trends and distinct events during the period studied. Benthic δ^{18}O values exhibit a consistent increasing trend during the late Eocene, indicating the overall decrease in oceanic bottom water temperatures. A sharp increase occurs at the

Eocene–Oligocene transition (between 33.9 and 33.3 Ma) at both sites examined. This rapid shift has been observed in several sites in the Southern Ocean (e.g. Muza et al., 1983; Miller et al., 1987; Mackensen and Ehrmann, 1992; Zachos et al., 1996; Billups et al., 2002; Pusz et al., 2011) and it is well established as a global signal (Zachos et al., 2001). It is generally interpreted as a combination of deep-ocean water cooling and major ice growth on the Antarctic continent (Zachos et al., 2001). At Site 689, the planktic δ^{18}O curve almost mimics the benthic one. The δ^{18}O values measured on fine fraction reveal a heavier trend more pronounced at ODP Site 748 (Kerguelen Plateau) compared to ODP Site 689 (Maud Rise). During the late Eocene, around 37 Ma, heavier δ^{18}O values are observed in both the Atlantic and Indian sectors of the SO, the benthic/fine-fraction ratio declines, indicating more homogenous temperature in the water column. Both benthic and planktic foraminifera δ^{13}C records show fluctuations across the period studied, with low values across the Eocene–Oligocene boundary, followed by an increase that accompanied the δ^{18}O increase and low values again in the upper Oligocene. The benthic trend is also observed by previous data from the same sites (Mackensen and Ehrmann, 1992; Diester-Haass and Zahn, 1996; Bohaty and Zachos, 2003). The fine-fraction records show elevated δ^{13}C values between the late Eocene and early Oligocene, followed by a decreasing trend during the Oligocene (from ca. 33.2 Ma). At Site 748, the fine-fraction δ^{13}C curve shows less fluctuation than the benthic curves during the middle late Eocene. A synchronous δ^{13}C increase (ca. 0.6 ‰ shift) is observed at 36.5 Ma. Elevated fine-fraction δ^{13}C values are observed from the late Eocene until the early Oligocene, coherent with previous studies (Bohaty and Zachos, 2003), while the benthic values stay low during the same period (Fig. 3d and f).

3.3 pCO_2 proxies

As noted above, given the complexities and potential biases of compiling data from different proxies and different time intervals, we prefer to use the single-site, single-proxy time series of pCO_2 from Zhang et al. (2013). These data (Fig. 4) show two peaks in the late Eocene, with a maximum for the entire study interval at ca. 37 Ma, a smaller peak at ca. 34.5 Ma, and a rapid drop of over 200 ppm from nearly 1000 to ca. 750 ppm in the earliest Oligocene (ca. 33.5 Ma). Despite the limitations of multi-proxy, multi-site compilations, the compiled data (Table S2, Fig. S7) show the same basic features, and the result does not appear to be sensitive to the precise choice of data to include in the analysis.

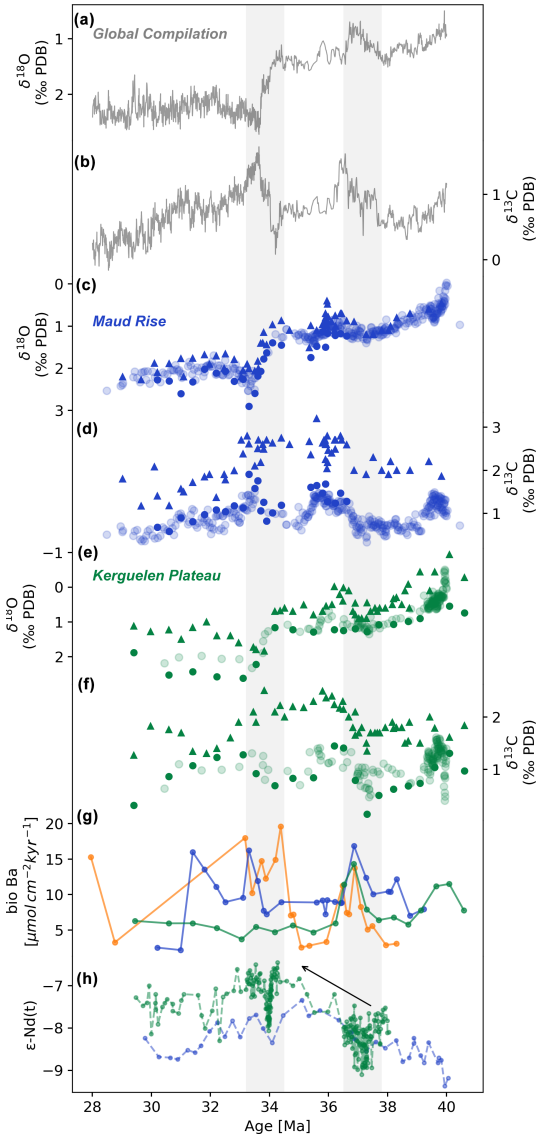

Figure 3. Multiproxy records from the late Eocene and early Oligocene. **(a, b)** Global compilation of oxygen and carbon stable isotopes (from Westerhold et al., 2020). **(c–f)** New generated oxygen and carbon benthic foraminiferal isotope data (solid circles) and fine fraction (< 45 µm) (solid triangles) and previously published oxygen and carbon stable isotopes (shaded circles, from Mackensen and Ehrmann, 1992; Diester-Haass and Zahn, 1996; Bohaty and Zachos, 2003) from the Atlantic sector of the Southern Ocean (Maud Rise) ODP Site 689 (in blue) and the Indian sector of the Southern Ocean (Kerguelen Plateau) ODP Site 748 (in green). PDB is Pee Dee Belemnite carbonate reference. **(g)** Biogenic barium (bio-Ba) export productivity (this study), with Site 689 in blue, Site 748 in green, and Site 1090 in orange. **(h)** Compilation of εNd data obtained from fossil fish teeth for the Atlantic sector of the SO (Maud Rise, in blue, Site 689) and for the Indian sector of the SO (Kerguelen Plateau, in green, Site 738 and Site 748) (Scher and Martin, 2004, 2006; Scher et al., 2014; Wright et al., 2018). The shaded area identifies the E–O boundary at ca. 33.8 Ma and productivity event at ca. 37 Ma. Note the inverted y axis scales for oxygen and Nd isotopes.

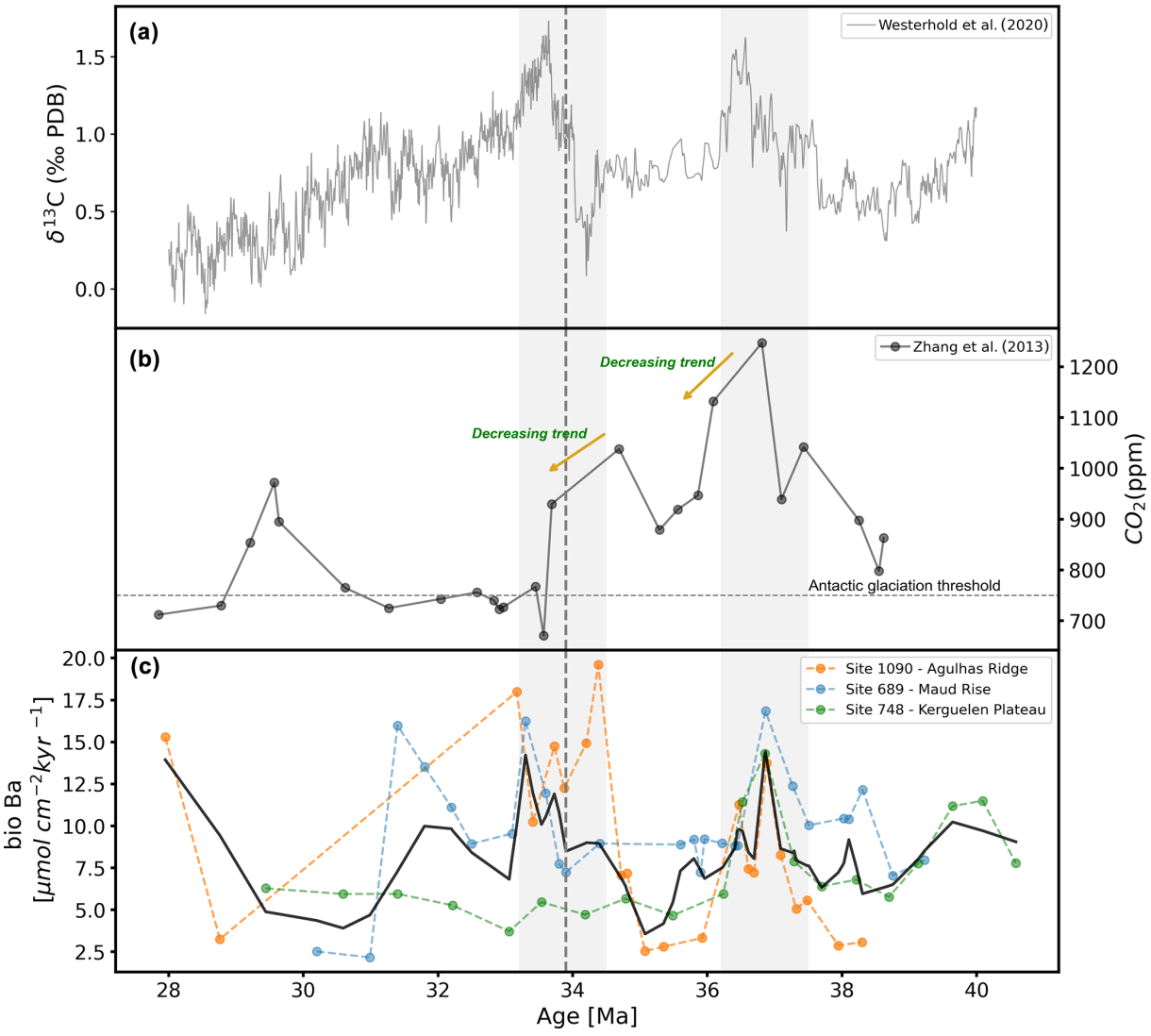

Figure 4. Comparison between **(a)** a global compilation of carbon stable isotopes (from Westerhold et al., 2020), **(b)** an alkenone-based atmospheric pCO_2 record (from Zhang et al., 2013), and **(c)** a biogenic barium (bio-Ba) export productivity proxy (this study). Antarctic glaciation thresholds (approx. 750 ppm) (from climate model, DeConto et al., 2008) is marked by a dashed line (horizontal). Shaded areas encompass the late Eocene and early Oligocene high-productivity intervals. The vertical dashed line identifies the E–O boundary (at ca. 33.8 Ma).

4 Discussion

4.1 Correlation of productivity to ocean circulation, glaciation and pCO_2 change

Intervals of high export productivity (bio-Ba) exhibit synchronous changes with intervals of changes in oxygen and carbon stable isotopes and pCO_2 data (Figs. 3 and 4). Notably, these intervals occur in the late Eocene (∼ 37 Ma) and at the E–O boundary (∼34 Ma). This correlation is highly suggestive that ocean circulation, glaciation, productivity, and atmospheric pCO_2 changes are interconnected. It could be assumed that (1) primary processes, such as ocean circulation and glaciation, are independently driving productivity and pCO_2 changes or that (2) a cascading effect, with glaciation and ocean circulation, is influencing productivity and consequently altering atmospheric pCO_2 levels. While we cannot in our study distinguish between these two possibilities, we explore the second, as proposed by Egan et al. (2013), in which changes in ocean conditions due to tectonic climate drivers affect productivity, and wherein the latter in turn affects pCO_2 levels.

4.2 The late Eocene productivity event and its potential impact

The noticeable bio-Ba AR peak at ∼ 36.8 Ma (Fig. 2) suggests an important ca. 1 Myr long event of approximate doubling of export productivity during the late Eocene, preceding the significant cooling and the first formation of large Antarctic ice sheets at the Eocene–Oligocene boundary. The temporal synchronicity among different site locations in the Southern Ocean suggests that the process driving this enhanced export productivity in the late Eocene occurred throughout the Southern Ocean, requiring a mechanism that increased the delivery of nutrients to the surface ocean.

Our findings corroborate previous paleoproductivity studies that indicate an increase in export productivity in the Atlantic sector of the Southern Ocean during this time period. Anderson and Delaney (2005) found several peaks in productivity indicators at the Agulhas Ridge during the same time interval, and benthic foraminiferal accumulation rates show an increase in paleo-primary productivity on Maud Rise (Diester-Haass and Faul, 2019) (Fig. 2). A pronounced opal abundance peak is also documented by Diekman et al. (2004) between 37.5 and 33.5 Ma at ODP Site 1090. Our results now show that the 37 Ma event extended at least as far as the Kerguelen Plateau in the Indian Ocean sector, with a substantial peak around 37 Ma and an earlier one near 40 Ma, thus affecting a large portion of the Southern Ocean region.

A direct analysis of the impact of the potential significance of this event for the development of late Eocene global climate depends on two key factors: the extent to which the increased productivity contributed to enhanced carbon sequestration, and the magnitude of sequestration over the ca. 1 Myr interval of enhancement. Understanding the impact of productivity on carbon sequestration for the Eocene oceans, however, is complicated by the lack of knowledge of several factors that influence this process. These factors include our ability to estimate the impact of higher productivity on carbon sequestration being limited, as many of the factors that affect this in the modern ocean are poorly understood for Eocene oceans (export efficiency to the subsurface waters, rates of transport and degradation in the water column and upper sediment layers, organic carbon content of Southern Ocean Eocene pelagic sediments, and transport of organic carbon by subsurface water layers in the late Eocene oceans to lower-latitude areas of productivity and sequestration). We therefore cannot directly calculate the impact that the observed productivity change had on pCO_2. Instead, we take an indirect approach, comparing the productivity history to the history of pCO_2 and potential drivers of productivity change such as ocean circulation and climate change.

4.3 Surface water changes in physical conditions in the late Eocene

The late Eocene is generally accepted as a time interval of gradual cooling of Southern Ocean waters. Indeed, biomarker-based temperature estimates reveal substantial (3–5 °C) high-latitude sea surface temperatures (SSTs) cooling within the late Eocene (Liu et al., 2009; O'Brien et al., 2020). Our fine-fraction stable oxygen isotopes confirm this cooling trend following MECO, with a distinct peak at 37 Ma during the Eocene, matching the peak cooling reported by O'Brien et al. (2020). This interval of maximum $\delta^{18}O$ values occurred during the same interval in which export productivity increased (Fig. 2). In this interval the difference in the $\delta^{18}O$ gradient between benthic foraminifera and fine-fraction (nannofossil) carbonate is less pronounced. This increase in similarity is interpreted as having been caused by a decrease in water column stratification and enhanced vertical mixing.

This change in export productivity in the late Eocene is coeval with a change towards increasing variability of carbon stable isotopes ($\delta^{13}C$) of benthic foraminifera (Fig. 4). Although $\delta^{13}C$ in individual sections can also represent local effects, usually there is a strong component of global changes in carbon reservoirs, and indeed our local measurements closely align with the global curve (Fig. 3b, d and f). In the global context, a shift towards more positive values in the benthic $\delta^{13}C$ at ∼ 37 Ma indicates a carbon cycle perturbation. This shift coincides with the export productivity changes observed in our study. One possible explanation is that higher productivity may have elevated the export flux of organic carbon to sediments, thereby increasing the marine organic carbon burial and preferentially scavenging the lighter ^{12}C from the carbon pool.

4.4 Oceanographic circulation drivers of the late Eocene productivity change

We propose that the main cause for the productivity increase observed in the late Eocene is the upwelling of nutrient-rich deep waters. However, understanding the physical oceanographic mechanisms that led to increased upwelling throughout the Southern Ocean requires examining links between the different processes that occurred at that time period. Changes in paleoceanography during the Paleogene were significantly mediated through tectonic re-organization, such as the Southern Ocean gateways opening (i.e. the Drake Passage and the Tasman Gateway) and changes in the Atlantic–Arctic gateway and in the Tethys Seaway.

In this context, the Southern Ocean circulation during this time period is still debated due to uncertainties concerning the opening of the gateways that led to the development of the Antarctic Circumpolar Current (ACC). Estimates for the onset of the modern-like ACC have not reached a consensus yet and vary from as early as the middle Eocene (ca. 41 Ma, Scher and Martin, 2006; ca. 35.5 Ma, Stickley et al.,

2004) to middle Oligocene (ca. 23 Ma; Pfuhl and McCave, 2005). This inconsistency suggests that the onset of ACC could have been a gradual or an intermittent change. Further, local proxy records cannot distinguish between regionally developed fronts and true circumpolar flow (i.e. ACC).

In addition to δ^{18}O and δ^{13}C, εNd has been used to identify circulation changes and water mass exchanges through the Eocene (Scher and Martin, 2004, 2008; Scher et al., 2014; Huck et al., 2017; Wright et al., 2018). Nd isotopes are one of the most robust tracers of water mass origin (Frank et al., 2002). The residence time of Nd in oceans is much shorter (300–1000 years) than ocean mixing time and is thus distinct at a given location. Further, the isotope composition of the Nd ocean budget is solely determined by terrigenous contribution. The latter is balanced by Nd sinks that remove Nd quantitatively, yet this only influences the net budget and thus the magnitude and/or swiftness of changes to the εNd composition. However, mixing of water masses, e.g. through lateral or vertical mixing, can also cause changes as long as they occur more rapidly than the residence times.

In the late Eocene, starting at 37 Ma, Scher and Martin (2004) found a dramatic positive shift in εNd values in the Atlantic sector of the SO that they interpreted as the influx of Pacific deep waters, due to its characteristic of more radiogenic (positive) waters, not previously observed in the Atlantic Ocean. Recently published Nd isotope records from the Kerguelen Plateau (Wright et al., 2018) revealed a long-term negative trend during the late Eocene, which also suggests that the water mass mixing between the Pacific and Atlantic preceded 36 Ma. εNd (t) records from the Kerguelen Plateau in fact showed values comparable to modern CDW during the Oligocene, inferring water mass composition similar to the present day. Thus, Nd isotope data support at least partial opening of Drake Passage by the late Eocene (before 36 Ma), consistent with plate tectonic reconstructions (Livermore et al., 2005, 2007). Regardless of the depth, neodymium isotope evidence for late Eocene opening of the Drake Passage suggests that increased fetch for surface flow and changing deep water composition could have had changes in the surface water conditions in the South Atlantic sector of the late Eocene Southern Ocean.

This has been explicitly demonstrated in a recent modelling study conducted by Toumoulin et al. (2020). They demonstrate that the Drake Passage opening, even at shallow depth, notably connects prior regional frontal systems together, thereby allowing the formation of a proto-ACC, and has a strong effect on the Southern Ocean Eocene water mass structure, inducing ocean cooling in most of the Southern Hemisphere. These temperature changes are not linear and differ from one region to another, with DP opening causing changes in the mixed-layer depths and provoking different responses in the Atlantic and Indian sectors of the SO. In the Atlantic and Indian ocean sectors in particular, very deep seasonal mixing (several hundred metres) over broad areas of the entire region is replaced by more moderate levels of mixing (generally ca. 200 m or less), except near the proto-polar front region, where seasonal mixing of 300–400 m still occurs. Villa et al. (2014) have found nannofossil assemblages characteristic of cool sea surface waters in the late Eocene in Kerguelen Plateau samples. Cooler temperatures are coeval with the paleoceanographic re-organization and intensified upwelling that we infer for this time period, while differences in the depth of the mixed layers between ocean basins may explain the different magnitude of export productivity observed in the Atlantic and Indian sectors of the SO.

The wind-driven eastward flow and the characteristic fronts of the modern ACC support the upwelling of nutrient-rich water to the surface and consequently high levels of productivity. On the balance of evidence, it seems that the export productivity seen in our data in the late Eocene is likely to have occurred in response to a proto-ACC front's development and its associated upwelling. The inferred onset of a proto-ACC in the late Eocene and our finding of increased upwelling fits the hypothesis that ACC type circulation itself helps drive the AMOC circulation (Toggweiler and Bjornsson, 2000; Katz et al., 2011; Sarkar et al., 2019). A proto-ACC causes SO upwelling, and thus provides support for increasing AMOC-like circulation in the late Eocene as an additional cause of increased upwelling as a causative mechanism of the export productivity event. Temperature asymmetry between Northern Hemisphere and Southern Hemisphere and comparisons between benthic δ^{13}C records provide evidence for the strengthening of the AMOC in the late Eocene (Elsworth et al., 2017).

4.5 Eocene–Oligocene boundary productivity changes

The earliest Oligocene, following the E–O boundary, has been suggested as a period of a significant rise in biological productivity in high southern latitudes (Diester-Haass, 1995, 1996; Diester-Haass and Zahn, 1996, 2001). However, in contrast to the late Eocene event, the export productivity changes across the Eocene–Oligocene boundary observed in our study were not always concurrent between the sites investigated (Fig. 2). In the Atlantic sites, export productivity increases and decreases several times from the late Eocene to early Oligocene. We thus argue that the fluctuations in export productivity that occurred in the Southern Ocean during this global climatic re-organization are more strongly modulated by local parameters, whereas the late Eocene productivity event is more uniform and reflects the global re-organization of ocean circulation. If the trends observed in export productivity across the EOT were regulated only by global, or at least regional temperature and circulation changes, then we would observe significant changes also in the Indian sector of the Southern Ocean. It seems, however, that productivity increase was more pronounced in the Atlantic sector of the Southern Ocean.

Today, the Southern Ocean (SO) has a frontal system that strongly impacts circulation, primary productivity, and the

entire climate system (Chapman et al., 2020). The Antarctic Polar Front (APF) is particularly important for controlling nutrient distribution. Latitudinal variations of the APF for example have been shown to alter regional productivity over the glacial cycles (Kim et al., 2014; Thole et al., 2019). The causes of the lack of significant export productivity changes in the Indian sector of the Southern Ocean during the early Oligocene after the Eocene–Oligocene boundary are unclear. The Kerguelen Plateau may not have been located in a position favourable to nutrient-rich upwelling. In addition, the regional frontal migration may have been more intense in the Atlantic sector compared to the Indian sector of the SO.

4.6 A scenario for Southern Ocean productivity and circulation change in the late Eocene

The patterns of productivity change seen in our study can be placed in an (admittedly speculative) scenario, which is at least compatible with prior studies and modelling of conditions in the late Eocene austral ocean region and Antarctica. In the earliest interval covered in our study (ca. 40–38 Ma) productivity was in most sites fairly low (Fig. 5a). At this time there is little evidence for a significant influx of Pacific waters into the Atlantic, and the Drake Passage is thus assumed to be effectively closed to ocean circulation.

During the 38–36 Ma interval, evidence summarized by Scher et al. (2014) suggests that a significant, if transient, glaciation event occurred on the Antarctic continent, i.e. the Priabonian oxygen maximum (PriOM). If it was sufficient in magnitude, this would have significantly affected circulation throughout the austral ocean region, with strengthened temperature gradients, invigorated circulation (Houben et al., 2019), and increased upwelling (Goldner et al., 2014). This would account both for the substantial increase in productivity and the broad geographic extent of the increase seen in our data (Fig. 5b). The cause of this glaciation event is unknown but may be related in part to the trend in the late Eocene towards lower atmospheric pCO_2 interacting with orbital fluctuations in polar insulation as explored in model simulations by Van Breedam et al. (2022).

With the end of transient glaciation, the atmospheric forcing of ocean circulation would have declined and with it the high levels of productivity seen in our data (Fig. 5c). However, by this time (ca. 36–34 Ma) the Nd isotope data suggests that a significant influx of Pacific water was reaching the South Atlantic sector of the austral ocean (Scher and Martin, 2004), and consequently the Drake Passage must have been at least partially open. This would have resulted in, if not as strong as during the PriOM, nonetheless stronger circumpolar circulation in a proto-ACC, increased upwelling, and increased nutrient availability from Pacific-sourced deep waters. The locus of high productivity, however, would have become more cantered near the proto-ACC, which at that time, according to the model results of Toumoulin et al. (2020), was located a few degrees north of the current location of the ACC. The high productivity and accumulation of biogenic opal seen at Site 1090, fortuitously located at this time in this region can be thus be explained, as can the lower relative productivity of Site 689, located much further to the south and thus outside the region primarily influenced by the proto-ACC system.

Lastly, at the E–O boundary itself (Fig. 5d), the well-known major shifts in oxygen isotopes signal the formation of a full continental ice sheet, which would have in turn driven a renewed increase in circumpolar ocean circulation, a full (if early) form of the ACC, and dramatically increased levels of productivity; however, these were again primarily near the ACC region.

4.7 Possible implications to the EOT global cooling

Our pCO_2 compilation shows that carbon dioxide levels declined gradually from ca. 1200 ppm in the late Eocene to ca. 750 ppm across the EOT (Figs. 4 and S7). There are different processes involved in the oceanic uptake of CO_2. The solubility pump is a physical–chemical process that promotes gas transfer between the atmosphere and seawater in order to achieve chemical equilibrium. This process depends on temperature, in which the solubility increases as temperature decreases. Evidence for cooling of surface waters observed in the Southern Ocean (Liu et al., 2009; Hutchinson et al., 2021) could have favoured the ability to dissolve atmospheric CO_2, contributing to the drawdown of pCO_2 during the late Eocene.

Silicate weathering has been suggested to play an essential role in regulating CO_2 across the EOT (Zachos and Kump, 2005). On geologic timescales, chemical silicate weathering is considered to modulate atmospheric CO_2 levels through a negative feedback mechanism (Berner et al., 1983). Weathering of silicate rocks provides alkalinity to the oceans, acting as a sink for atmospheric CO_2, thereby influencing global climate. In addition, increasing silicate weathering enhances primary productivity through the delivery of nutrients to the ocean. Intensified weathering is supported by marine Os isotopic ($^{187}Os/^{188}Os$) isotope records, showing an anomaly before the EOT, at ca. 35.5 Ma (Dalai et al., 2006).

High export productivity potentially modulates CO_2 by two major mechanisms, operating over very different timescales. Productivity maintains a gradient in dissolved CO_2 between the surface and deep ocean by exporting organic carbon from the surface into deep-ocean waters. This in turn lowers the concentration of CO_2 in surface waters, causing more atmospheric CO_2 to be drawn out of the atmosphere into dissolved surface ocean CO_2. It is estimated that this mechanism causes pCO_2 to be approximately 200 ppm lower than it would in a purely abiotic ocean (Volk and Hoffert 1985). In the second mechanism, in areas of the ocean with high export productivity a (generally rather small) fraction of biologically captured carbon (both soft tissue and carbonate from coccolithophores and planktic foraminifera) es-

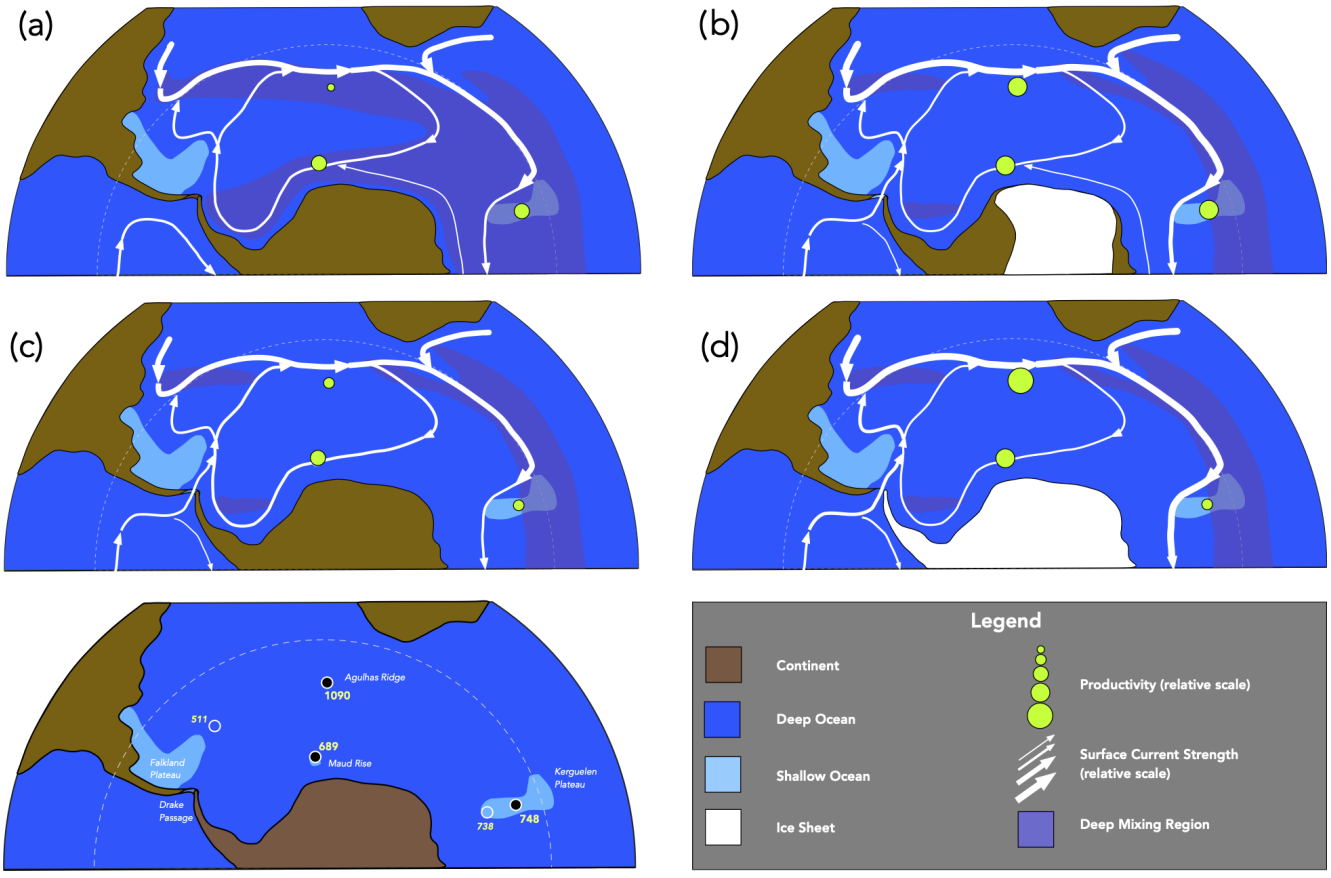

Figure 5. Interpretive scenario of palaeoceanographic changes in the late Eocene to early Oligocene Southern Ocean. Base map, circulation patterns, and extent of deep mixing regions after Toumoulin et al. (2020), with ice sheet extent at 38 Ma after models in Van Breedam et al. (2022). Productivity values based on results of this study, shown in relative scale. Note the general trend towards higher productivity values, and within this the higher productivity focussed near proto-ACC during intervals with inferred ice sheets.

capes remineralization in the water column and is buried in ocean bottom sediments, where it is sequestered for (typically) many millions of years. Changes in either mechanism can contribute to the decline of atmospheric carbon dioxide, thereby intensifying the cooling trend. Therefore, the observed increase in export productivity in the late Eocene over 1 Myr in multiple sites in the SO, and the temporal correlation with the changes in pCO_2 proxy records showed in our study is compatible with the hypothesis proposed by Egan et al. (2013). This suggests that the heightened export productivity identified in our study is a potential candidate that may have provided important positive feedback to the pCO_2 decline.

However, this correlation is suggestive rather than conclusive, given the complexities of the carbon cycle. For instance, variations in the efficiency of the carbon pump, remineralization (Griffith et al., 2021), the relationship between nutrient availability and plankton utilization, and the dynamics of shelf-deep sea carbonate (Sluijs et al., 2013) can significantly influence the relationship between export productivity and pCO_2 levels and add complexity to our understanding. Limited data for the late Eocene regarding some of the critical parameters required for our understanding (e.g. sedimentary C_{org}, Olivarez Lyle and Lyle, 2006) further contributes to the uncertainties in establishing a causal link. Moreover, it is essential to note that upwelling, while promoting nutrient-rich conditions favourable to productivity and the long-term sequestration mechanism, also contribute to outgassing of CO_2 into atmosphere, influencing the carbon balance in the short-term mechanism. This adds another layer of complexity to the carbon cycle dynamics and its relationship with productivity changes. While our findings propose a potential link, it is crucial to recognize that this alone does not constitute proof that the export productivity directly influenced late Eocene pCO_2 levels.

Despite some modelling studies showing that circulation changes were not the main factor in driving the cooling and glaciation on Antarctica (e.g. Huber et al., 2004; Huber and Nof, 2006; Sijp et al., 2011), circulation changes still had a significant impact, with, for example, Southern Ocean sea surface temperature declines of 2–4 °C (Toumoulin et al., 2020) affecting the atmosphere–ocean CO_2 equilibrium. A

succession of events may have contributed to the evolution of climate: thermal isolation of Antarctica, glacier formation, increasing intensity of silicate weathering, together with upwelling of nutrient-rich and cold deep waters, leading to high biological productivity and then declining pCO_2. Moreover, because the Atlantic Meridional Overturning Circulation (AMOC) affects the distribution of tracers such as temperature, dissolved inorganic carbon (DIC), alkalinity, and nutrients (Boot et al., 2022), the strengthening of AMOC could explain the further decrease in atmospheric CO_2 via biological export productivity. Elsworth et al. (2017), for example, suggest that enhanced weathering is driven by intensified AMOC in the latest Eocene due to increasing AMOC causing differential global distribution and an increase in surface temperatures and precipitation over land areas. These factors together suggest that E–O changes in AMOC also may play an important role as a driver of CO_2 decline.

Taken together, the above processes indicate that a variety of positive feedback contributed to Antarctic glaciation from about 37 Ma onwards. Recent evidence suggests that continental-scale Antarctic glaciation initiated in the late Eocene (Scher et al., 2014; Carter et al., 2017). Our results indicate that significant changes in Southern Ocean export productivity preceded the E–O boundary by approximately 3 million years. These trends are likely to be a response to the combination of the intensified processes that had been in place since the late Eocene. The correlation between our Southern Ocean productivity peaks and decline in global pCO_2 records suggest that biological productivity may have played an important role in the drawdown of pCO_2 levels. Specifically enhanced CO_2 fixation by phytoplankton and carbon sequestration in seafloor sediments increased via an increase in the biological pump may have contributed to decrease atmospheric CO_2, and through a positive feedback from declining Southern Ocean surface water temperature enhanced boosting the cooling trend. The establishment of Antarctic glaciation may thus have been influenced significantly by enhanced productivity.

4.8 Limitations and future directions

Our study has numerous limitations. Our data on paleoproductivity does not cover the full time interval in all of the sites studied, and our geographic coverage is still incomplete. In particular, we have not examined sections from the Pacific sector, or the influence of the Tasman gateway. Most of our interpretations are based on a single productivity proxy – biogenic barium. While this proxy is well established and gives coherent results in our study, productivity proxies are known to have complex behaviours, and results using different proxies might be at least somewhat different. Our suggestion that elevated late Eocene Southern Ocean productivity might have affected global carbon sequestration is only a speculation based on general characteristics of the ocean carbon system, and a much more detailed study of both actual sequestration values in sediment and the impact on atmospheric pCO_2 is still needed. Our interpretative scenario attributing productivity changes to a combination of Drake Passage opening and continental-scale glaciation in Antarctica are also purely qualitative and need further study. Despite these limitations, our study sheds new light on the late Eocene oceanic precursors of the Eocene–Oligocene glaciation event, which was the most dramatic climate change of the Cenozoic.

5 Conclusions

Our bio-Ba data provide important records of the Southern Ocean productivity history across the EOT. These data show that export productivity increased significantly in the late Eocene in the Southern Ocean and was affected by ocean circulation changes. The development of a regionally varying circumpolar polar flow (proto-ACC) and the associated frontal system proposed by other recent studies is likely to have contributed to the enhanced productivity in the Southern Ocean through the intensification of upwelling (H1).

Our results show that increasing Southern Ocean productivity in the late Eocene to earliest Oligocene is correlated to global changes in atmospheric pCO_2 and carbon isotope proxies for organic carbon extraction. This finding points toward a potential positive climate system feedback, involving ocean circulation changes, enhanced export productivity, and drawdown of atmospheric CO_2. Although many studies of the Eocene–Oligocene climate transition try to identify a single dominant mechanism (e.g. ocean gateway opening versus pCO_2 decline) for causing the initiation of Antarctica glaciation, each mechanism plays a different role and has associated complex feedbacks. Our study points toward a climate feedback system involving ocean circulation, thermal isolation, and biological productivity, where several mechanisms are interconnected and cannot be considered separately. Openings of gateways led to the development of a circumpolar flow, promoting cooling, and increased upwelling that contributed to enhanced ocean carbon pump activity and the decline of atmospheric carbon dioxide.

Data availability. The supplementary information related to this article is available in the Supplement, and the raw data will be available upon publication in an open-access database (PANGAEA: https://doi.pangaea.de/10.1594/PANGAEA.959619 (Faria et al., 2024).

Supplement. The supplement related to this article is available online at: https://doi.org/10.5194/cp-20-1327-2024-supplement.

Author contributions. The manuscript was designed and written by GRF in collaboration with DL. DL updated age models.

GRF prepared all the samples for geochemical analyses. JS ran the barium and aluminium analyses. US generated carbon and oxygen-stable isotope data. pCO_2 data and neodymium isotopes data were compiled by GRF. Biogenic barium was calculated by GRF. All authors contributed to editing the manuscript.

Competing interests. The contact author has declared that none of the authors has any competing interests.

Disclaimer. Publisher's note: Copernicus Publications remains neutral with regard to jurisdictional claims made in the text, published maps, institutional affiliations, or any other geographical representation in this paper. While Copernicus Publications makes every effort to include appropriate place names, the final responsibility lies with the authors.

Acknowledgements. The authors thank Sylvia Dietze of the MfN for sample preparation, Jeremy Young of UCL for advice on nannofossils, and the journal editor and reviewers for their time and many valuable suggestions.

Financial support. This research has been supported by the Bundesministerium für Bildung, Wissenschaft, under the "Make our Planet Great Again, German Research Initiative" implemented by the German Academic Exchange Service (DAAD) grant no. 57429681.

The publication of this article was funded by the Open Access Fund of the Leibniz Association.

Review statement. This paper was edited by Arne Winguth and reviewed by Peter Bijl and one anonymous referee.

References

Anagnostou, E., John, E. H., Edgar, K. M., Foster, G. L., Ridgwell, A., Inglis, G. N., Pancost, R. D., Lunt, D. J., and Pearson, P. N.: Changing atmospheric CO_2 concentration was the primary driver of early Cenozoic climate, Nature, 533, 380–384, https://doi.org/10.1038/nature17423, 2016.

Anagnostou, E., John, E. H., Babila, T. L., Sexton, P. F., Ridgwell, A., Lunt, D. J., Pearson, P. N., Chalk, T. B., Pancost, R. D. and Foster, G. L.: Proxy evidence for state-dependence of climate sensitivity in the Eocene greenhouse, Nat. Commun., 11, 4436, https://doi.org/10.1038/s41467-020-17887-x, 2020.

Anderson, J. B., Warny, S., R. A. Askin, J. S. Wellner, S. M. Bohaty, A. E. Kirshner, D. N. Livsey, A. R. Simms, T. R. Smith, W. Ehrmann, L. A. Lawver, D. Barbeau, S. W. Wise, D. K. Kulhanek, F. M. Weaver, and Majewski, W..: Progressive Cenozoic cooling and the demise of Antarctica's last refugium, P. Natl. Acad. Sci. USA, 108, 11356–11360, https://doi.org/10.1073/pnas.1014885108, 2011.

Anderson, L. D. and Delaney, M. L.: Middle Eocene to early Oligocene paleoceanography from Agulhas Ridge, Southern Ocean (Ocean Drilling Program Leg 177, Site 1090), Paleoceanography and Paleoclimatology, 20, 1, https://doi.org/10.1029/2004PA001043, 2005.

Archer, D., Winguth, A., Lea, D., and Mahowald, N.: What caused the glacial/interglacial atmospheric pCO_2 cycles?, Rev. Geophys., 38, 159–189, https://doi.org/10.1029/1999RG000066, 2000.

Arrhenius, S.: On the influence of carbonic acid in the air upon the temperature of the ground, Philosophical Magazine and Journal of Science, 5, 237–276, 1896.

Aubry, M. P.: Late Paleogene Calcareous nannoplankton evolution: a tale of climatic deterioration, in: Eocene/Oligocene Climatic and Biotic Evolution, edited by: Prothero, D. R. and Berggren, W. A., Princeton University Press, Princeton, NJ, 272–309, https://doi.org/10.1515/9781400862924.272, 1992.

Baatsen, M., von der Heydt, A. S., Huber, M., Kliphuis, M. A., Bijl, P. K., Sluijs, A., and Dijkstra, H. A.: The middle to late Eocene greenhouse climate modelled using the CESM 1.0.5, Clim. Past, 16, 2573–2597, https://doi.org/10.5194/cp-16-2573-2020, 2020.

Baldauf, J. G. and Barron, J. A.: Diatom biostratigraphy: Kerguelen Plateau and Prydz Bay regions of the Southern Ocean, in: Proceedings of the Ocean Drilling Program, Scientific Results (Ocean Drilling Program), edited by: Barron, J., Larsen, B., et al., College Station, TX, 119, 547–598, https://doi.org/10.2973/odp.proc.sr.119.135.1991, 1991.

Barker, P. and Thomas, E.: Origin, signature and palaeoclimatic influence of the Antarctic Circumpolar Current, Earth-Sci. Rev., 66, 143–162, 2004.

Barker, P. E., Kennett, J. P., et al.: Proc. ODP, Init. Repts., 113, Ocean Drilling Program, College Station, TX, https://doi.org/10.2973/odp.proc.ir.113, 1988.

Barker, P. F.: Scotia Sea regional tectonic evolution: implications for mantle flow and palaeocirculation, Earth-Sci. Rev., 55, 1–39, https://doi.org/10.1016/S0012-8252(01)00055-1, 2001.

Barron, J., Larsen, B., et al.: Proc. ODP, Init. Repts., 119, Ocean Drilling Program, College Station, TX, https://doi.org/10.2973/odp.proc.ir.119.1989, 1989.

Beerling, D. and Royer, D.: Convergent Cenozoic CO_2 history, Nat. Geosci., 4, 418–420, https://doi.org/10.1038/ngeo1186, 2011.

Berggren, W. A., Kent, D. V., Swisher III, C. C., and Aubry, M. P.: A revised Cenozoic geochronology and chronostratigraphy, in: Geochronology, time scales and global stratigraphic correlation: Framework for an historical geology, edited by: Berggren, W. A., Berggren, W. A., Kent, D. V., Aubry, M.-P., and Hardenbol, J.: SEPM (Society for Sedimentary Geology) Special Publication 54, 129–212, https://doi.org/10.2110/pec.95.04.0129, 1995.

Berner, R. A., Lasaga, A. C. and Garrels, R. M.: The carbonate-silicate geochemical cycle and its effect on atmospheric carbon dioxide over the past 100 million years, Am. J. Sci., 283, 641–683, https://doi.org/10.2475/ajs.283.7.641, 1983.

Billups, K., Channell, J. E. T., and Zachos, J.: Late Oligocene to early Miocene geochronology and paleoceanography from the subantarctic South Atlantic, Paleoceanography, 17, 1004, https://doi.org/10.1029/2000PA000568, 2002.

Bohaty, S. M. and Zachos, J. C.: Significant Southern Ocean warming event in the late middle Eocene, Geology, 31, 1017–1020, https://doi.org/10.1130/G19800.1, 2003.

Bohaty, S. M., Zachos, J. C., and Delaney, M. L.: Foraminiferal Mg/Ca evidence for Southern Ocean cooling across the Eocene–Oligocene transition, Earth Planet. Sc. Lett., 317–318, 251–261, https://doi.org/10.1016/j.epsl.2011.11.037, 2012.

Bokhari, S. N. H. and Meisel, T. C.: Method development and optimisation of sodium peroxide sintering forgGeological samples, Geostand. Geoanalyt. Res., 41, 181–195, https://doi.org/10.1111/ggr.12149, 2016.

Boot, A., von der Heydt, A. S., and Dijkstra, H. A.: Effect of the Atlantic Meridional Overturning Circulation on atmospheric pCO_2 variations, Earth Syst. Dynam., 13, 1041–1058, https://doi.org/10.5194/esd-13-1041-2022, 2022.

Brandt, A., Bathmann, U., Brix, S., Cisewski, B., Flores, H., Göcke, C., Janussen, D., Krägefsky, S., Kruse, S., Leach, H., Linse, K., Pakhomov, E., Peeken, I., Riehl, T., Sauter, E., Sachs, O., Schüller, M., Schrödl, M., Schwabe, E., Strass, V., van Franeker, J. A., and Wilmsen, E.: Maud Rise – A snapshot through the water column, Deep-Sea Res. Pt. II, 58, 1962–1982, https://doi.org/10.1016/j.dsr2.2011.01.008, 2011.

Carter, A., Riley, T. R., Hillenbrand, C. D., and Rittner, M.: Widespread Antarctic glaciation during the Late Eocene, Earth Planet. Sc. Lett., 458, 49–57, https://doi.org/10.1016/j.epsl.2016.10.045, 2017.

Carter, L., McCave, I. N., and Williams, M. J. M.: Chapter 4 Circulation and Water Masses of the Southern Ocean: A Review, in: v. 8, Developments in Earth and Environmental Sciences, Elsevier, 85–114, https://doi.org/10.1016/S1571-9197(08)00004-9, 2008.

Channell, J. E. T., Galeotti, S., Martin, E. E., Billups, K., Scher, H. D., and Stoner, J. S.: Eocene to Miocene magnetostratigraphy, biostratigraphy and chemostratigraphy at ODP Site 1090 (sub-Antarctic South Atlantic), Geol. Soc. Am. Bull., 115, 607–623, 2003.

Chapman, C. C., Lea, M. A., and Meyer, A.: Defining Southern Ocean fronts and their influence on biological and physical processes in a changing climate. Nature Climate Change, 10, 209–219, https://doi.org/10.1038/s41558-020-0705-4, 2020.

Cooke, P. J., Nelson, C. S., Crundwell, M. P., and Spiegler, D.: *Bolboforma* as monitors of Cenozoic palaeoceanographic changes in the Southern Ocean, Palaeogeogr. Palaeocl., 188, 73–100, https://doi.org/10.1016/S0031-0182(02)00531-X, 2002.

Coxall, H. K. and Pearson, P. N.: The Eocene-Oligocene Transition, in: Deep-Time Perspectives on Climate Change: Marrying the Signal from Computer Models and Biological Proxies, edited by: Williams, M., Haywood, A. M., Gregory, J., and Schmidt, D. N., Micropaleontology Society Special Publication, Geological Society, London, 351–387, ISBN 9781862392403, 2007.

Coxall, H. K. and Wilson, P. A.: Early Oligocene glaciation and productivity in the eastern equatorial Pacific: Insights into global carbon cycling, Paleoceanography, 26, PA2221, https://doi.org/10.1029/2010PA002021, 2011.

Coxall, H. K., Wilson, P. A., Pälike, H., Lear, C. H., and Backman, J.: Rapid stepwise onset of Antarctic glaciation and deeper calcite compensation in the Pacific Ocean, Nature, 433, 53–57, https://doi.org/10.1038/nature03135, 2005.

Cramer, B. S., Toggweiler, J. R., Wright, J. D., Katz, M. E., and Miller, K. G.: Ocean overturning since the Late Cretaceous: Inferences from a new benthic foraminiferal isotope compilation, Paleoceanography, 24, 1–14, https://doi.org/10.1029/2008PA001683, 2009.

Dalai, T., Ravizza, G., and Peucker-Ehrenbrink, B.: The Late Eocene $^{187}Os/^{188}Os$ excursion: Chemostratigraphy, cosmic dust flux and the Early Oligocene glaciation, Earth Planet. Sc. Lett., 241, 477–492, https://doi.org/10.1016/j.epsl.2005.11.035, 2006.

De Baar, H., de Jong, J. T. M., Bakker, D. C. E., Löscher, B. M., Veth, C., Bathmann, U., and Smetacek, V.: Importance of iron for plankton blooms and carbon dioxide drawdown in the Southern Ocean, Nature, 373, 412–415, https://doi.org/10.1038/373412a0, 1995.

DeConto, R. and Pollard, D.: Rapid Cenozoic glaciation of Antarctica induced by declining atmospheric CO_2, Nature, 421, 245–249, https://doi.org/10.1038/nature01290, 2003.

DeConto, R. M., Pollard, D., Wilson, P. A., Palike, H., Lear, C. H., and Pagani, M.: Thresholds for Cenozoic bipolar glaciation, Nature, 455, 652–656, https://doi.org/10.1038/nature07337, 2008.

Deppeler, S. L. and Davidson, A. T.: Southern Ocean Phytoplankton in a Changing Climate, Front. Mar. Sci., 4, 40, https://doi.org/10.3389/fmars.2017.00040, 2017.

DeVries, T.: The Ocean Carbon Cycle, Annu. Rev. Env. Resour., 47, 317–341, https://doi.org/10.1146/annurev-environ-120920-111307, 2022.

Diekmann, B., Kuhn, G., Gersonde, R., and Mackensen, A.: Middle Eocene to early Miocene environmental changes in the sub-Antarctic Southern Ocean: Evidence from biogenic and terrigenous depositional patterns at ODP site 1090, Global Planet. Change, 40, 295–313, https://doi.org/10.1016/j.gloplacha.2003.09.001, 2004.

Diester-Haass, L.: Late Eocene–Oligocene sedimentation in the Antarctic Ocean, Atlantic Sector (Maud Rise, ODP leg 113, Site 689), Development of surface and bottom water circulation, in: The Antarctic Paleoenvironment: A Perspective on Global Change, Part 1, Antarct. Res. Ser., vol. 56, edited by: Kennett, J. P., and Warnke, D. A., Am. Geophys. Un., Washington, D.C., 185–202, https://doi.org/10.1029/AR056p0185, 1992.

Diester-Haass, L.: Middle Eocene to early Oligocene Paleoceanography of the Antarctic Ocean (Maud Rise, ODP Leg 113, Site 689): change from a low to a high productivity ocean, Palaeogeogr. Palaeocl., 113, 311–334, https://doi.org/10.1016/0031-0182(95)00067-V, 1995.

Diester-Haass, L.: Late Eocene–Oligocene paleoceanography in the southern Indian Ocean (ODP Site 744), Mar. Geol., 130, 99–119, 1996.

Diester-Haass, L. and Faul, K.: Paleoproductivity reconstructions for the Paleogene Southern Ocean: A direct comparison of geochemical and micropaleontological proxies, Paleoceanography and Paleoclimatology, 34, 79–97, https://doi.org/10.1029/2018PA003384, 2019.

Diester-Haass, L. and Zachos, J.: The Eocene–Oligocene transition in the Equatorial Atlantic (ODP Site 925); paleoproductivity increase and positive d13C excursion, in: From greenhouse to icehouse; the marine Eocene–Oligocene transition, edited by: Prothero, D. R., Ivany, L. C., and Nesbitt, E. A., Columbia University Press, New York, NY, USA, https://doi.org/10.1144/TMS002.16, 2003.

Diester-Haass, L. and Zahn, R.: Eocene–Oligocene transition in the Southern Ocean: History of water mass circulation and biological productivity, Ge-

ology, 24, 163–166, https://doi.org/10.1130/0091-7613(1996)024<0163:EOTITS>2.3.CO;2, 1996.

Diester-Haass, L. and Zahn, R.: Paleoproductivity increase at the Eocene–Oligocene climatic transition: ODP/DSDP Sites 763 and 592, Palaeogeogr. Palaeocl., 172, 153–170, https://doi.org/10.1016/S0031-0182(01)00280-2, 2001.

Douglas, P. M. J., Affek, H. P., Ivany, L. C., Houben, A. J. P., Sijp, W. P., Sluijs, A., Schouten, S., and Pagani, M.: Pronounced zonal heterogeneity in Eocene southern high-latitude sea surface temperatures, P. Natl. Acad. Sci. USA, 111, 6582–6587, https://doi.org/10.1073/pnas.1321441111, 2014.

Dutkiewicz, A. and Müller, R. D.: The carbonate compensation depth in the South Atlantic Ocean since the Late Cretaceous, Geology, 49, 873–878, https://doi.org/10.1130/G48404.1, 2021.

Dymond, J., Suess, E., and Lyle, M.: Barium in Deep-Sea Sediment: A Geochemical Proxy for Paleoproductivity, Paleoceanography and Paloclimatology, 7, 163–181, https://doi.org/10.1029/92PA00181, 1992.

Egan, K. E., Rickaby, R. E. M., Hendry, K. R., and Halliday, A. N.: Opening the gateways for diatoms primes Earth for Antarctic glaciation, Earth Planet. Sc. Lett., 375, 34–43, https://doi.org/10.1016/J.EPSL.2013.04.030 , 2013.

Elsworth, G., Galbraith, E., Halverson, G., and Yang, S.: Enhanced weathering and CO_2 drawdown caused by latest Eocene strengthening of the Atlantic meridional overturning circulation, Nat. Geosci., 10, 213–216, https://doi.org/10.1038/ngeo2888, 2017.

Faria, G. R., Lazarus, D. B., Renaudie, J., Stammeier, J., Özen, V., and Struck, U.: Late Eocene to early Oligocene oxygen and carbon isotope records and biogenic barium accumulation rates in Maud Rise, Kerguelen Plateau and Agulhas Ridge [dataset bundled publication], PANGAEA [data set], https://doi.org/10.1594/PANGAEA.959619, 2024.

Faul K. L. and Delaney, M. L.: A comparison of early Paleogene export productivity and organic carbon burial flux for Maud Rise, Weddell Sea, and Kerguelen Plateau, south Indian Ocean, Paleoceanography, 25, 3214, https://doi.org/10.1029/2009PA001916, 2010.

Florindo, F. and Roberts, A. P.: Eocene–Oligocene magnetobiochronology of ODP Sites 689 and 690, Maud Rise, Weddell Sea, Antarctica, Geol. Soc. Am. Bull., 117, 46–66, https://doi.org/10.1130/b25541.1, 2005.

Frank, M., Whiteley, N., Kasten, S., Hein, J. R., and O'Nions, K.: North atlantic deep water export to the southern ocean over the past 14 Myr: Evidence from Nd and Pb isotopes in ferromanganese crusts, Paleoceanography, 17, 12-1–12-9, https://doi.org/10.1029/2000PA000606, 2002.

Galeotti, S., Coccioni, R., and Gersonde, R.: Middle Eocene–Early Pliocene Subantarctic planktic foraminiferal biostratigraphy of Site 1090, Agulhas Ridge, Mar. Micropaleontol., 45, 357–381, https://doi.org/10.1016/S0377-8398(02)00035-X., 2002.

Gasson, E., Lunt, D. J., DeConto, R., Goldner, A., Heinemann, M., Huber, M., LeGrande, A. N., Pollard, D., Sagoo, N., Siddall, M., Winguth, A., and Valdes, P. J.: Uncertainties in the modelled CO_2 threshold for Antarctic glaciation, Clim. Past, 10, 451–466, https://doi.org/10.5194/cp-10-451-2014, 2014.

Gersonde, R., Hodell, B. A., Blum, P., and Shipboard Scientific Party: Leg 177 summary, Proc. Ocean Drill. Program, Initial Rep., 177, 1–67, 1999.

Glass, B. P., Hall, C. M., and York, D.: $^{40}Ar/^{39}Ar$ laser probe dating of North American tektite fragments from Barbados and the age of the Eocene–Oligocene boundary, Chem. Geol., 59, 181–186, https://doi.org/10.1016/0168-9622(86)90070-9, 1996.

Goldner, A., Herold, N., and Huber, M.: Antarctic glaciation caused ocean circulation changes at the Eocene–Oligocene transition, Nature, 511, 574–577, https://doi.org/10.1038/nature13597, 2014.

Gradstein, F. M., Ogg, J. G., Schmitz, M., and Ogg, G.: The Geological Time Scale 2012, Elsevier, Oxford, UK, 1176 pp., ISBN 9780444594488, 2012.

Griffith, E. M., Thomas, E., Lewis, A. R., Penman, D. E., Westerhold, T., and Winguth, M. E.: Bentho-Pelagic Decoupling: The Marine Biological Carbon Pump During Eocene Hyperthermals, Paleoceanogr. Paleoclim., 36, e2020PA004053, https://doi.org/10.1029/2020PA004053, 2021.

Gruetzner, J. and Uenzelmann-Neben, G.: Contourite drifts as indicators of Cenozoic bottom water intensity in the eastern Agulhas Ridge area, South Atlantic, Mar. Geol., 378, 350–360, https://doi.org/10.1016/j.margeo.2015.12.003, 2016.

Hill, D. J., Haywood, A. M., Valdes, P. J., Francis, J. E., Lunt, D. J., Wade, B. S., and Bowman, V. C.: Paleogeographic controls on the onset of the Antarctic circumpolar current, Geophys. Res. Lett., 40, 5199–5204, 2013.

Houben, A. J. P., van Mourik, C. A., Montanari, A., Coccioni, R., and Brinkhuis, H.: The Eocene–Oligocene transition: Changes in sea level, temperature or both?, Palaeogeogr. Palaeocl., 335–336, 75–83, https://doi.org/10.1016/j.palaeo.2011.04.008, 2012.

Houben, A. J. P., Bijl, P. K., Sluijs, A., Schouten, S., and Brinkhuis, H.: Late Eocene Southern Ocean cooling and invigoration of circulation preconditioned Antarctica for full scale glaciation, Geochem. Geophy. Geosy., 20, 2214–2234, https://doi.org/10.1029/2019GC008182, 2019.

Huber, B. T. and Quillevere, F.: Revised Paleogene Planktonic Foraminiferal biozonation for the Austral realm, J. Foramin. Res., 35, 299–314, https://doi.org/10.2113/35.4.299, 2005.

Huber, M. and Nof, D.: The ocean circulation in the southern hemisphere and its climatic impacts in the Eocene, Palaeogeogr. Palaeocl., 231, 9–28, https://doi.org/10.1016/j.palaeo.2005.07.037, 2006.

Huber, M., Brinkhuis, H., Stickley, C. E., Döös, K., Sluijs, A., Warner, J., Schellenberg, S. A., and Williams, G. L.: Eocene circulation of the Southern Ocean: Was Antarctica kept warm by subtropical waters?, Paleoceanography, 19, PA4026, https://doi.org/10.1029/2004PA001014, 2004.

Huck, C. E., van de Flierdt, T., Bohaty, S. M., and Hammond, S. J.: Antarctic climate, Southern Ocean circulation patterns, and deep-water formation during the Eocene, Paleoceanography, 32, 674–691, https://doi.org/10.1002/2017PA003135, 2017.

Hutchinson, D. K., Coxall, H. K., Lunt, D. J., Steinthorsdottir, M., de Boer, A. M., Baatsen, M., von der Heydt, A., Huber, M., Kennedy-Asser, A. T., Kunzmann, L., Ladant, J.-B., Lear, C. H., Moraweck, K., Pearson, P. N., Piga, E., Pound, M. J., Salzmann, U., Scher, H. D., Sijp, W. P., Śliwińska, K. K., Wilson, P. A., and Zhang, Z.: The Eocene–Oligocene transition: a review of marine and terrestrial proxy data, models and model–data comparisons, Clim. Past, 17, 269–315, https://doi.org/10.5194/cp-17-269-2021, 2021.

Inglis, G. N., Farnsworth, A., Lunt, D., Foster, G. L., Hollis, C. J., Pagani, M., Jardine, P. E., Pearson, P. N., Markwick, P., Galsworthy, A. M. J., Raynham, L., Taylor, K. W. R., and Pancost, R. D.: Descent toward the Icehouse: Eocene sea surface cooling inferred from GDGT distributions, Paleoceanography, 30, 1000–1020, https://doi.org/10.1002/2014PA002723, 2015.

Inokuchi, H. and Heider, F.: Paleolatitude of the southern Kerguelen Plateau inferred from the paleomagnetic study of late Cretaceous basalts, in: Proceedings of the Ocean Drilling Program, Scientific Results, edited by: Wise, S. W., Schlich, R., et al.: Ocean Drilling Program, College Station, TX, 120, 89–96, https://doi.org/10.2973/odp.proc.sr.120.129.1992, 1992.

IPCC: Climate Change 2021: The Physical Science Basis, in: Contribution of Working Group I to the Sixth Assessment Report of the Intergovernmental Panel on Climate Change, edtied by: Masson-Delmotte, V., Zhai, P., Pirani, A., Connors, S. L., Péan, C., Berger, S., Caud, N., Chen, Y., Goldfarb, L., Gomis, M. I., Huang, M., Leitzell, K., Lonnoy, E., Matthews, J. B. R., Maycock, T. K., Waterfield, T., Yelekçi, O., Yu, R., and Zhou, B., Cambridge University Press, Cambridge, UK and New York, NY, USA, https://doi.org/10.1017/9781009157896, in press, 2021.

Katz, M. E., Cramer, B. S., Toggweiler, J. R., Esmay, G., Liu, C., Miller, K. G., Rosenthal, Y., Wade, B. S., and Wright, J. D.: Impact of Antarctic Circumpolar Current Development on Late Paleogene Ocean Structure, Science, 332, 1076–1079, https://doi.org/10.1126/science.1202122, 2011.

Kennet, J. P.: Cenozoic evolution of Antarctic glaciation, the circum-Antarctic Ocean, and their impact on global paleoceanography, J. Geophys. Res., 82, 3843–3860, https://doi.org/10.1029/JC082i027p03843, 1977.

Kennett, J. P. and Stott, L. D.: Proteus and Proto-Oceanus: ancestral Paleogene oceans as revealed from antarctic stable isotopic results: ODP Leg 113, in: Leg 113. ODP Sci. Res., 865–880, https://doi.org/10.2973/odp.proc.sr.113.188.1990, 1990.

Kim, J. H., Crosta, X., Michel, E., Schouten, S., Duprat, J., and Damsté, J. S. S.: Impact of lateral transport on organic proxies in the Southern Ocean, Quatern. Res., 71, 246–250, https://doi.org/10.1016/j.yqres.2008.10.005, 2009.

Kim, Y. S. and Orsi, A. H.: On the Variability of Antarctic Circumpolar Current Fronts Inferred from 1992–2011 Altimetry, J. Phys. Oceanogr., 44, 3054–3071, https://doi.org/10.1175/JPO-D-13-0217.1, 2014.

Kuhlbrodt, T., Griesel, A., Montoya, M., Levermann, A., Hofmann, M., and Rahmstorf, S.: On the driving processes of the Atlantic meridional overturning circulation, Rev. Geophys., 45, RG2001, https://doi.org/10.1029/2004RG000166, 2007.

Kürschner, W. M., Kvaček, Z., and Dilcher, D. L.: The impact of Miocene atmospheric carbon dioxide fluctuations on climate and the evolution of terrestrial ecosystems, P. Natl. Acad. Sci. USA, 105, 449–453, https://doi.org/10.1073/pnas.0708588105, 2008.

Ladant, J.-B., Donnadieu, Y., and Dumas, C.: Links between CO_2, glaciation and water flow: reconciling the Cenozoic history of the Antarctic Circumpolar Current, Clim. Past, 10, 1957–1966, https://doi.org/10.5194/cp-10-1957-2014, 2014.

Lauretano, V., Kennedy-Asser, A. T., Korasidis, V. A., Wallace, M. W., Valdes, P. J., Lunt, D. J., Pancost, R. D. and Naafs, B. D. A.: Eocene to Oligocene terrestrial Southern Hemisphere cooling caused by declining pCO_2, Nat. Geosci., 14, 659–664, https://doi.org/10.1038/s41561-021-00788-z, 2021.

Lazarus, D. and Caulet, J. P.: Cenozoic Southern Ocean reconstructions from sedimentologic, radiolarian, and other microfossil data, in: The Antarctic Paleoenvironment: A perspective on global change. Pt. 2, Antarctic Research Series, 60, edited by: Kennett, J. P. and Warnke, D. A., AGU, 145–174, ISBN 10:0875908381, 1994.

Li, Z., Lozier, M. S., and Cassar, N.: Linking Southern Ocean Mixed Layer Dynamics to Net Community Production on Various Timescales, J. Geophys. Res.-Oceans, 126, e2021JC017537, https://doi.org/10.1029/2021JC017537, 2021.

Liu, Z., Pagani, M., Zinniker, D., DeConto, R., Huber, M., Brinkhuis, H., Shah, S. R., Leckie, R. M., and Pearson, A.: Global cooling during the Eocene–Oligocene climate transition, Science, 323, 1187–1190, https://doi.org/10.1126/science.1166368, 2009.

Livermore, R., Nankivell, A., Eagles, G., and Morris, P.: Paleogene opening of Drake Passage, Earth Planet. Sc. Lett., 236, 459–470, https://doi.org/10.1016/j.epsl.2005.03.027, 2005.

Livermore, R., Hillenbrand, C., Meredith, M., and Eagles, G.: Drake Passage and Cenozoic climate: an open and shut case?, Geochem. Geophy. Geosy., 8, Q01005, https://doi.org/10.1029/2005GC001224, 2007.

Lyle, M., Gibbs, S., Moore, T. C., and Rea, D. K.: Late Oligocene initiation of the Antarctic circumpolar current: evidence from the South Pacific, Geology, 35, 691–694, 2007.

Mackensen, A. and Ehrmann, W. U.: Middle Eocene through Early Oligocene climate history and paleoceanography in the Southern Ocean: Stable oxygen and carbon isotopes from ODP Sites on Maud Rise and Kerguelen Plateau, Mar. Geol., 108, 1–27, https://doi.org/10.1016/0025-3227(92)90210-9, 1992.

Marino, M. and Flores, J. A.: Middle Eocene to early Oligocene calcareous nannofossil stratigraphy at Leg 177 Site 1090, Mar. Micropaleontol., 45, 383–398, https://doi.org/10.1016/S0377-8398(02)00036-1, 2002.

Martin, E. E. and Haley, B. A.: Fossil fish teeth as proxies for seawater Sr and Nd isotopes, Geochim. Cosmochim. Ac., 64, 835–847, https://doi.org/10.1016/S0016-7037(99)00376-2, 2000.

Martin, E. E. and Scher, H. D.: Preservation of seawater Sr and Nd isotopes in fossil fish teeth: bad news and good news, Earth Planet. Sc. Lett., 220, 25–39, https://doi.org/10.1016/S0012-821X(04)00030-5, 2004.

Mikolajewicz, U., Maier-Reimer, E., Crowley, T. J., and Kim, K.-Y.: Effect of Drake and Panamanian Gateways on the circulation of an ocean model, Paleoceanography, 8, 409–426, https://doi.org/10.1029/93PA00893, 1993.

Miller, K. G., Janecek, T. R., Katz, M. E., and Keil, D. J.: Abyssal circulation and benthic foraminiferal changes near the Paleocene/Eocene boundary, Paleoceanography, 2, 741–761, https://doi.org/10.1029/PA002i006p00741, 1987.

Moore, J. K., Abbott, M. R., Richman, J. G., Smith, W. O., Cowles, T. J., Coale, K. H., Gardner, W. D., and Barber, R. T.: SeaWiFS satellite ocean color data from the Southern Ocean, Geophys. Res. Lett., 26, 1465–1468, 1999.

Muza, J. P., Williams, D. F., and Wise, S. W.: Paleogene oxygen record for Deep Sea Drilling Project Sites 511 and 512, subantarctic South Atlantic Ocean: Paleotemperatures, paleoceanographic changes, and the Eocene/Oligocene boundary event, in: Initial Reports of the Deep-Sea Drilling Project, edited by: Ludwig, W. J., Krasheninnikov, V.

A., et al., U. S. Govt. Printing Office, 71, 409–422, https://doi.org/10.2973/dsdp.proc.71.117.1983, 1983.

Najjar, R. G., Nong, G. T., Seidov, D., and Peterson, W. H.: Modelling geographic impacts on early Eocene ocean temperature, Geophys. Res. Lett., 29, 401–404, https://doi.org/10.1029/2001GL014438, 2002.

Nelson, D. M. and Smith, W.: Sverdrup revisited: Critical depths, maximum chlorophyll levels, and the control of Southern Ocean productivity by the irradiance-mixing regime, Limnol. Oceanogr., 36, 1650–1661, https://doi.org/10.4319/lo.1991.36.8.1650, 1991.

Nielsen, E. B., Anderson, L. D., and Delaney, M. L.: Paleoproductivity, nutrient burial, climate change and the carbon cycle in the western equatorial Atlantic across the Eocene/Oligocene boundary, Paleoceanography, 18, 1057, https://doi.org/10.1029/2002PA000804, 2003.

Nooteboom, P. D., Baatsen, M., Bijl, P. K., Kliphuis, M. A., van Sebille, E., Sluijs, A., Dijkstra, H. A., and von der Heydt, A. S.: Improved Model-Data Agreement With Strongly Eddying Ocean Simulations in the Middle-Late Eocene, Paleoceanography and Paleoclimatology, 37, e2021PA004405, https://doi.org/10.1029/2021PA004405, 2022.

O'Brien, C. L., Huber, M., Thomas, E., Pagani, M., Super, J. R., Elder, L. E., and Hull, P. M.: The enigma of Oligocene climate and global surface temperature evolution, P. Natl. Acad. Sci. USA, 117, 25302–25309, https://doi.org/10.1073/pnas.2003914117, 2020.

Olivarez Lyle, A. and Lyle, M. W.: Missing organic carbon in Eocene marine sediments: Is metabolism the biological feedback that maintains end-member climates?, Paleoceanography, 21, PA2007, https://doi.org/10.1029/2005PA001230, 2006.

Orsi, A. H., Whitworth, T., and Nowlin, W. D.: On the meridional extent and fronts of the Antarctic Circumpolar Current, Deep-Sea Res. Pt. I, 42, 641–673, https://doi.org/10.1016/0967-0637(95)00021-W, 1995.

Pagani, M., Zachos, J. C., Freeman, K. H., Tipple, B., and Bohaty, S.: Marked decline in atmospheric carbon dioxide concentrations during the Paleogene, Science, 309, 600–603, https://doi.org/10.1126/science.1110063, 2005.

Pagani, M., Huber, M., Liu, Z., Bohaty, S. M., Henderiks, J., Sijp, W., Krishnan, S., and DeConto, R. M.: The role of carbon dioxide during the onset of Antarctic glaciation, Science, 334, 1261–1264, https://doi.org/10.1126/science.1203909, 2011.

Pälike, H., Lyle, M. W., Nishi, H., Raffi, I., Ridgwell, A., Gamage, K., Klaus, A., Acton, G., Anderson, L., Backman, J., Baldauf, J., Beltran, C., Bohaty, S. M., Bown, P., Busch, W., Channell, J. E. T., Chun, C. O. J., Delaney, M., Dewangan, P., Dunkley Jones, T., Edgar, K. M., Evans, H., Fitch, P., Foster, G. L., Gussone, N., Hasegawa, H., Hathorne, E. C., Hayashi, H., Herrle, J. O., Holbourn, A., Hovan, S., Hyeong, K., Iijima, K., Ito, T., Kamikuri, S., Kimoto, K., Kuroda, J., Leon-Rodriguez, L., Malinverno, A., Moore, T. C., Murphy, B. H., Murphy, D. P., Nakamura, H., Ogane, K., Ohneiser, C., Richter, C., Robinson, R., Rohling, E. J., Romero, O., Sawada, K., Scher, H., Schneider, L., Sluijs, A., Takata, H., Tian, J., Tsujimoto, A., Wade, B. S., Westerhold, T., Wilkens, R., Williams, T., Wilson, P. A., Yamamoto, Y., Yamamoto, S., Yamazaki, T., and Zeebe, R. E.: A Cenozoic record of the equatorial Pacific carbonate compensation depth, Nature, 488, 609–615, https://doi.org/10.1038/nature11360, 2012.

Palter, J. B., Marinov, I., Sarmiento, J. L., and Gruber, N.: Large-Scale, Persistent Nutrient Fronts of the World Ocean: Impacts on Biogeochemistry, in: Chemical Oceanography of Frontal Zones, The Handbook of Environmental Chemistry, Vol. 116, edited by: Belkin, I. M., Springer, Berlin, Heidelberg, https://doi.org/10.1007/698_2013_241, 2013, 2013.

Persico, D. and Villa, G.: Eocene–Oligocene calcareous nannofossils from Maud Rise and Kerguelen Plateau (Antarctica): Palaeoecological and palaeoceanographic implications, Mar. Micropaleontol., 52, 153–179, https://doi.org/10.1016/j.marmicro.2004.05.002, 2004.

Pfuhl, H. A. and McCave, I. N.: Evidence for late Oligocene establishment of the Antarctic Circumpolar Current, Earth Planet. Sc. Lett., 235, 715–728, 2005.

Piepgras, D. J. and Wasserburg, G. J.: Isotopic composition of neodymium in waters from the drake passage, Science, 217, 207–214, https://doi.org/10.1126/science.217.4556.207, 1982.

Prothero, D. R. and Berggren, W. A.: Eocene–Oligocene Climatic and Biotic Evolution, Princeton University Press, Princeton, NJ, ISBN 0691604959, 1992.

Pusz, A. E., Thunell, R. C., and Miller, K. G.: Deep water temperature, carbonate ion, and ice volume changes across the Eocene–Oligocene climate transition, Paleoceanography, 26, PA2205, https://doi.org/10.1029/2010PA001950, 2011.

Rea, D. K. and Lyle, M. W.: Paleogene calcite compensation depth in the eastern subtropical Pacific: Answers and questions, Paleoceanography, 20, PA1012, https://doi.org/10.1029/2004PA001064, 2005.

Renaudie, J., Lazarus, D., and Diver, P.: NSB (Neptune Sandbox Berlin): An expanded and improved database of marine planktonic microfossil data and deep-sea stratigraphy, Palaeontol. Electron., 23, a11, https://doi.org/10.26879/1032, 2020.

Retallack, G. J.: Refining a pedogenic-carbonate CO_2 paleobarometer to quantify a middle Miocene greenhouse spike, Palaeogeogr. Palaeocl., 281, 57–65, 2009.

Rintoul, S. R., Hughes, C. W., and Olbers, D.: Chapter 4.6 – The antarctic circumpolar current system, in: book series: International Geophysics, v.77, 271-XXXVI, edited by: Siedler, G., Church, J., and Gould, J., Academic Press, ISBN 9780126413519, https://doi.org/10.1016/S0074-6142(01)80124-8, 2001.

Robert, C., Diester Haass, L. and Chamley, H.: Late Eocene Oligocene oceanographic development at southern high latitudes, from terrigenous and biogenic particles: A comparison of Kerguelen Plateau and Maud Rise, ODP Sites 744 and 689, Mar. Geol., 191, 37–54, https://doi.org/10.1016/S0025-3227(02)00508-X, 2002.

Roberts, A. P., Bicknell, S. J., Byatt, J., Bohaty, S. M., Florindo, F., and Harwood, D. M.: Magnetostratigraphic calibration of Southern Ocean diatom datums from the Eocene–Oligocene of Kerguelen Plateau (Ocean Drilling Program Sites 744 and 748), Palaeogeogr. Palaeocl., 198, 145–168, https://doi.org/10.1016/S0031-0182(03)00397-3, 2003.

Roberts, N. L., Piotrowski, A. M., McManus, J. F., and Keigwin, L. D.: Synchronous deglacial overturning and water mass source changes, Science, 327, 75–78, https://doi.org/10.1126/science.1178068, 2010.

Salamy, K. A. and Zachos, J. C.: Latest Eocene-early Oligocene climate change and Southern Ocean fertility: inferences

from sediment accumulation and stable isotope data, Palaeogeogr. Palaeoclim., 145, 61–77, https://doi.org/10.1016/S0031-0182(98)00093-5, 1999.

Sarkar, S., Basak, C., and Frank, M.: Late Eocene onset of the Proto-Antarctic Circumpolar Current, Sci. Rep.-UK, 9, 10125, https://doi.org/10.1038/s41598-019-46253-1, 2019.

Sarmiento, J. L., Gruber, N., Brzezinski, M. A., and Dunne, J. P.: High-latitude controls of thermocline nutrients and low latitude biological productivity, Nature, 247, 56–60, https://doi.org/10.1038/nature02127, 2004.

Sauermilch, I., Whittaker, J. M., Klocker, A., Munday, D. R., Hochmuth, K., Bijl, P. K., and LaCasce, J. H.: Gateway-driven weakening of ocean gyres leads to Southern Ocean cooling, Nat. Commun., 12, 6465, https://doi.org/10.1038/s41467-021-26658-1, 2021.

Scher, H. D., Whittaker, J. M., Williams, S. E., Latimer, J. C., Kordesch, W. E. C., and Delaney, M. L.: Onset of Antarctic Circumpolar Current 30 million years ago as Tasmanian Gateway aligned with westerlies, Nature, 523, 580–583, https://doi.org/10.1038/nature14598, 2015.

Scher H. D. and Delaney M. L.: Breaking the glass ceiling for high resolution Nd isotope records in early Cenozoic paleoceanography, Chem. Geol., 269, 329–338, https://doi.org/10.1016/j.chemgeo.2009.10.007, 2010.

Scher, H. D. and Martin, E. E.: Circulation in the Southern Ocean during the Paleogene inferred from neodymium isotopes, Earth Planet. Sc. Lett., 228, 391–405, https://doi.org/10.1016/J.EPSL.2004.10.016, 2004.

Scher, H. D. and Martin, E. E.: Oligocene deep water export from the North Atlantic and the development of the Antarctic Circumpolar Current examined with neodymium isotopes, Paleoceanography, 23, PA1205, https://doi.org/10.1029/2006PA001400, 2008.

Scher, H. D. and Martin, E. E.: Timing and climatic consequences of the opening of Drake Passage, Science, 312, 428–430, https://doi.org/10.1126/science.1120044, 2006.

Scher, H. D., Bohaty, S. M., Zachos, J. C., and Delaney, M. L.: Two-stepping into the icehouse: East Antarctic weathering during progressive ice-sheet expansion at the Eocene–Oligocene transition, Geology, 39, 383–386, https://doi.org/10.1130/G31726.1, 2011.

Scher, H. D., Bohaty, S. M., Smith, B. W., and Munn, G. H.: Isotopic interrogation of a suspected late Eocene glaciation, Paleoceanography 29, 628–644, https://doi.org/10.1002/2014PA002648, 2014.

Schumacher, S. and Lazarus, D.: Regional differences in pelagic productivity in the late Eocene to early Oligocene – a comparison of southern high latitudes and lower latitudes, Palaeogeogr. Palaeocl., 214, 243–263, https://doi.org/10.1016/j.palaeo.2004.06.018, 2004.

Seton, M., Müller, R., Zahirovic, S., Gaina, C., Torsvik, T., Shephard, G., Talsma, A., Gurnis, M., Turner, M., Maus, S., and Chandler, M.: Global continental and ocean basin reconstructions since 200 Ma, Earth-Sci. Rev., 113, 212–270, https://doi.org/10.1016/j.earscirev.2012.03.002, 2012.

Shackleton, N. J. and Kennett, P.: Paleotemperature history of the Cenozoic and the initiation of Antarctic glaciation: Oxygen and carbon isotope analysis in DSDP Sites 277, 279 and 281, Initial Rep. Deep Sea, 29, 881–884, 1975.

Shackleton, N. J. and Opdyke, N. D.: Oxygen isotope and paleomagnetic stratigraphy of equatorial Pacific core V28-238: Oxygen isotope temperatures and ice volumes on a 105 year and 106 year scale, Quatern. Res., 3, 39–55, https://doi.org/10.1016/0033-5894(73)90052-5, 1973.

Shackleton, N. J., Hall, M. A., and Boersma, A.: Oxygen and carbon isotope data from Leg 74 foraminifers, Initial Rep. Deep Sea, 74, 599–612, 1984.

Sigman, D., Hain, M., and Haug, G.: The polar ocean and glacial cycles in atmospheric CO_2 concentration, Nature, 466, 47–55, https://doi.org/10.1038/nature09149, 2010.

Sigman, D. M. and Boyle, E. A.: Glacial/interglacial variations in atmospheric carbon dioxide, Nature, 407, 859–869, https://doi.org/10.1038/35038000, 2000.

Sijp, W. P., England, M. H., and Toggweiler, J. R.: Effect of Ocean Gateway Changes under Greenhouse Warmth, J. Climate, 22, 6639–6652, https://doi.org/10.1175/2009JCLI3003.1, 2009.

Sijp, W. P., England, M. H., and Huber, M.: Effect of the deepening of the Tasman Gateway on the global ocean, Paleoceanography, 26, 1–18, https://doi.org/10.1029/2011PA002143, 2011.

Sijp, W. P., von der Heydt, A. S., and Bijl, P. K.: Model simulations of early westward flow across the Tasman Gateway during the early Eocene, Clim. Past, 12, 807–817, https://doi.org/10.5194/cp-12-807-2016, 2016.

Sluijs, A., Zeebe, R. E., Bijl, P. K., and Bohaty, S. M.: A middle Eocene carbon cycle conundrum, Nat. Geosci., 6, 429–434, https://doi.org/10.1038/ngeo1807, 2013.

Sokolov, S. and Rintoul, S. R.: Multiple jets of the Antarctic Circumpolar Current south of Australia, J. Phys. Oceanogr., 37, 1394–1412, 2007.

Sokolov, S. and Rintoul, S. R.: Circumpolar structure and distribution of the Antarctic Circumpolar Current fronts: 1. Mean circumpolar paths, J. Geophys. Res., 114, C11018, https://doi.org/10.1029/2008JC005108, 2009.

Spiess, V.: Cenozoic magnetostratigraphy of Leg 113 drill sites, Maud Rise, Weddell Sea, Antarctica, in: Proceedings of the Ocean Drilling Program, Scientific Results, v. 113, edited by: Barker, P. F., et al., College Station, Texas, 261–318, https://doi.org/10.2973/odp.proc.sr.113.182.1990, 1990.

Steinthorsdottir, M., Porter, A. S., Holohan, A., Kunzmann, L., Collinson, M., and McElwain, J. C.: Fossil plant stomata indicate decreasing atmospheric CO_2 prior to the Eocene–Oligocene boundary, Clim. Past, 12, 439–454, https://doi.org/10.5194/cp-12-439-2016, 2016.

Stickley, C. E., Brinkhuis, H., Schellenberg, S. A., Sluijs, A., Röhl, U., Fuller, M., Grauert, M., Huber, M., Warnaar, J., and Williams, G. L.: Timing and nature of the deepening of the Tasmanian Gateway, Paleoceanography, 19, 4, https://doi.org/10.1029/2004PA001022, 2004.

Taylor, V. E., Westerhold, T., Bohaty, S. M., Backman, J., Dunkley Jones, T., Edgar, K. M.. Egan, K. E., Lyle, M., Pälike, H., Röhl, U., Zachos, J., and Wilson, P. A.: Transient Shoaling, Over-Deepening and Settling of the Calcite Compensation Depth at the Eocene–Oligocene Transition, Paleoceanography and Paleoclimatology, 38, e2022PA004493, https://doi.org/10.1029/2022PA004493, 2023.

The Cenozoic CO_2 Proxy Integration Project ($CENCO_2PIP$) Consortium: Toward a Cenozoic History of Atmospheric CO_2,

Science, 382, eadi5177, https://doi.org/10.1126/science.adi5177, 2023.

Thole, L. M., Amsler, H. E., Moretti, S., Auderset, A., Gilgannon, J., Lippold, J., Vogel, H., Crosta, X., Mazaud, A., Michel, E., Martínez-García, A., and Jaccard, S. L.: Glacial–Interglacial dust and export production records from the Southern Indian Ocean, Earth Planet. Sc. Lett., 525, 115716, https://doi.org/10.1016/j.epsl.2019.115716, 2019.

Thomas, E.: Late Cretaceous through Neogene deep-sea benthic foraminifera (Maud Rise, Weddell Sea, Antarctica), Proc. Ocean Drill. Program Sci. Results, 113, 571–594, 1990.

Toggweiler, J. R. and Bjornsson, H.: Drake Passage and palaeoclimate, J. Quaternary Sci., 15, 319–328, https://doi.org/10.1002/1099-1417(200005)15:4<319::AID-JQS545>3.0.CO;2-C, 2000.

Toggweiler, J. R. and Samuels, B.: Effect of Drake Passage on the global thermohaline circulation, Deep-Sea Res. Pt. I, 42, 477–500, 1995.

Toumoulin, A., Donnadieu, Y., Ladant, J., Batenburg, S. J., Poblete, F., and Dupont-Nivet, G.: Quantifying the Effect of the Drake Passage Opening on the Eocene Ocean, Paleoceanography and Paleoclimatology, 35, e2020PA003889, https://doi.org/10.1029/2020PA003889, 2020.

Van Breedam, J., Huybrechts, P., and Crucifix, M.: Modelling evidence for late Eocene Antarctic glaciations, Earth Planet. Sc. Lett., 586, 117532, https://doi.org/10.1016/j.epsl.2022.117532, 2022.

Villa, G., Fiorini, C., Persico, D., Roberts, A. P., and Florindo, F.: Middle Eocene to Late Oligocene Antarctic glaciation/deglaciation and Southern Ocean productivity, Paleoceanography and Paloclimatology, 29, 223–237, https://doi.org/10.1002/2013PA002518, 2014.

Volk, T. and Hoffert, M. I.: Ocean carbon pumps: analysis of relative strengths and efficiencies in ocean-driven atmospheric CO_2 changes, in: The carbon cycle and atmospheric CO_2: natural variations Archean to present, Chapman conference papers, 1984, Geophysical Monograph 32, edited by: Sundquist, E. T. and Broecker, W. S., American Geophysical Union, 99–110, 1985.

Vonhof, H. B., Smit, J., Brinkhuis, H., Montanari, A., and Nederbragt, A. J.: Global cooling accelerated by early late Eocene impacts, Geology, 28, 687–690, https://doi.org/10.1130/0091-7613(2000)0282.3.CO;2, 2000.

Wei, W.: Paleogene chronology of Southern Ocean drill holes: An update, in: The Antarctic paleoenvironment: A perspective on global change, Antarctic Research Series, edited by: Kennett, J. P. and Warnke, D. A., 75–96, ISBN 9781118667781, https://doi.org/10.1029/AR056, 1992.

Wei, W. and Wise Jr., S. W.: Eocene–Oligocene calcareous nannofossil magnetobiochronology of the Southern Ocean, Newsl. Stratigr., 26, 119–132, 1992.

Westerhold, T., Marwan, N., Drury, A. J., Liebrand, D., Agnini, C., Anagnostou, E., Barnet, J. S. K., Bohaty, S. M., Vleeschouwer, Florindo, F., Frederichs, T., Hodell, D. A., Holbourn, A. E., Kroon, D., Lauretano, V., Littler, K., Lourens, L. J., Lyle, M., Pälike, H., Röhl, U., Tian, J., Wilkens, R. H., Wilson, P. A. and Zachos, J. C.: An astronomically dated record of Earth's climate and its predictability over the last 66 million years, Science, 369, 6509, 1383–1387, https://doi.org/10.1126/science.aba6853, 2020.

Wright, N. M., Scher, H. D., Seton, M., Huck, C. E., and Duggan, B. D.: No change in Southern Ocean Circulation in the Indian Ocean from the Eocene through Late Oligocene, Paleoceanography, Paleoclimatology, 33, 152–167, https://doi.org/10.1002/2017PA003238, 2018.

Zachos, C. J., Quinn, T. M., and Salamy, K. A.: High-resolution (104 years) deep-sea foraminiferal stable isotope records of the Eocene–Oligocene climate transition, Paleoceanography, 11, 251–266, 1996.

Zachos, C. J., Opdyke, B. N., Quinn, T. M., Jones, C. E., and Halliday, A. N.: Early Cenozoic glaciation, Antarctic weathering, and seawater $^{87}Sr/^{86}Sr$: Is there a link?, Chem. Geol., 161, 165–180, 1999.

Zachos, J. and Kump, L.: Carbon cycle feedbacks and the initiation of Antarctic glaciation in the earliest Oligocene, Global Planet. Change, 47, 51–66, https://doi.org/10.1016/j.gloplacha.2005.01.001, 2005.

Zachos, J., Pagani, M., Sloan, L., Thomas, E., and Billups, K.: Trends, rhythms and aberrations in global climate 65 Ma to present, Science, 292, 686–693, https://doi.org/10.1126/science.1059412, 2001.

Zhang, Y. G., Pagani, M., Liu, Z., Bohaty, S. M., and DeConto, R.: A 40-million-year history of atmospheric CO_2, Philos. T. R. Soc. A, 371, 20130096, https://doi.org/10.1098/rsta.2013.0096, 2013.